



Stability Analyses of the 1981 San Luis Dam Slide

Ashok K. Chugh, Civil Engineer, U.S. Bureau of Reclamation, Denver, CO 80225, USA; email:

achugh@usbr.gov

D.V. Griffiths, Professor, Colorado School of Mines, Golden, CO 80401, USA; email: d.v.griffiths@mines.edu

ABSTRACT: *The 1981 upstream slope failure in San Luis Dam in California, USA, is analyzed for stability and deformations in two- and three-dimensions using continuum-mechanics-based analysis procedures implemented in the computer programs FLAC and FLAC3D. The analysis results (failure surface, factor of safety, and displacements) from the continuum models are in general agreement with the field data. In addition, two-dimensional slope stability analysis results using a modified form of limit-equilibrium-based Spencer's procedure for variable factor of safety implemented in the computer program SSTAB2 are included. Overall, the analysis results supplement the previously reported failure analyses. The paper serves three primary functions: (1) it documents results of a different analysis of the 1981 San Luis Dam slope failure; (2) it demonstrates the use of 2-D and 3-D continuum models to study the onset of instability, failure surface geometry and location, and permanent displacements associated with slope failures; and (3) it demonstrates the use of variable factor of safety to identify location of instability initiation, and progression of instability in a soil deposit. In addition, the paper demonstrates the benefits of three-dimensional analysis for complex conditions in dam engineering practice.*

KEYWORDS: analysis; case history; dams; failure; slope stability; two- and three- dimensional numerical analysis

SITE LOCATION: [IJGCH-database.kmz](#) (requires Google Earth)

NOTE: Imperial units were used on this project. The data and analyses reported in this paper were converted, wherever practicable, to metric units and rounded. The numerical information contained in this paper should, therefore, be interpreted keeping in mind this change of units.

INTRODUCTION

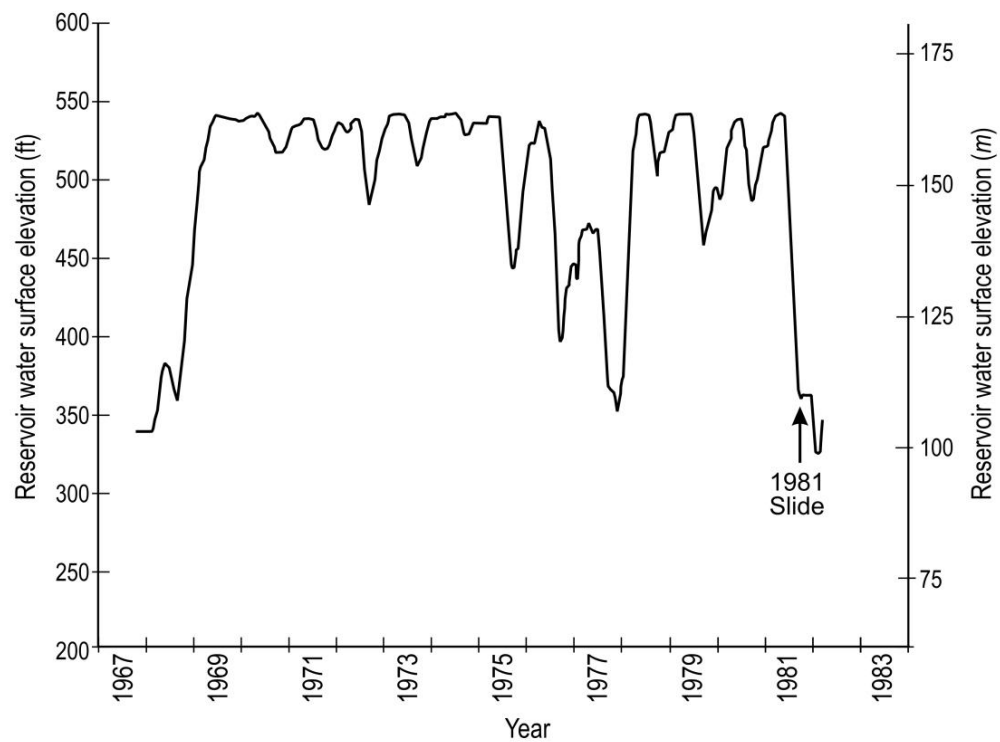
In 1981, San Luis Dam (now known as B.F. Sisk Dam) in California, USA experienced a deep seated slope failure in the upstream (u/s) slope. The construction of the dam was completed in 1967. It is an off-stream, pumped-storage facility and as such the dam is frequently subjected to significant fluctuations in reservoir water level (RWL). The slope failure had occurred during an unprecedented drawdown of the RWL by about 55 m (180 ft) in 120 days. Following the slide, field investigations, laboratory tests, and stability analyses were performed to understand the cause(s) of the failure. Figure 1(a) shows the significant portion of the slide and scarp, and Figure 1(b) shows the reservoir operational history leading up to the slide. Figure 2 shows the longitudinal profile view along the centerline of the dam crest – figures 1(a) and 2 are limited to the reach of the slide; total length of the dam is 5.6-km (3.5-mile). The dam was remediated in 1982 by construction of a large buttress against the u/s slope and the facility has performed satisfactorily since.

Submitted: 29 May 2015; Published: 10 December 2015

Reference: Chugh A.K. and Griffiths D.V. (2015). *Stability Analyses of the 1981 San Luis Dam Slide*. International Journal of Geoengineering Case histories, <http://casehistories.geoengineer.org>, Vol.3, Issue 2, p.85-112. doi: 10.4417/IJGCH-03-02-03

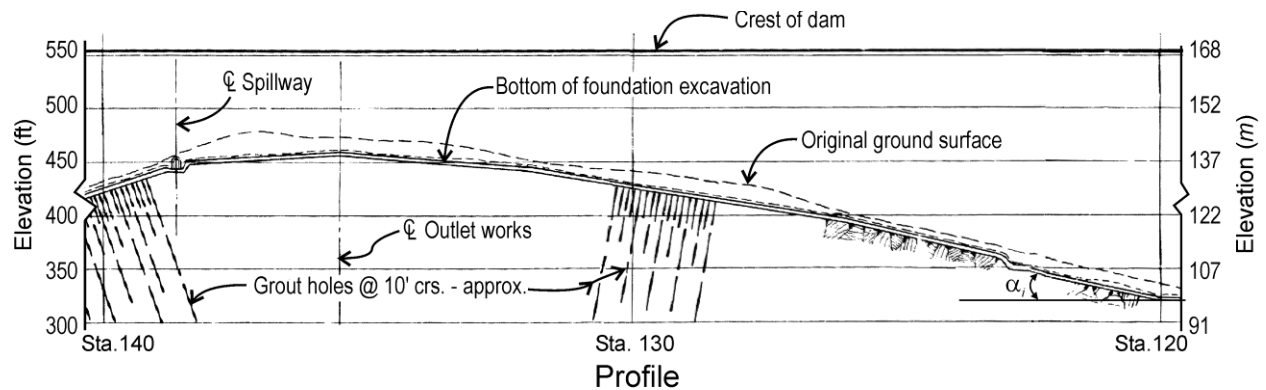


(a)



(b)

Figure 1. San Luis Dam site: (a) Elevation view of the 1981 slide; (b) Reservoir operational history.



Sta. station;
 α_i natural ground slope angle for $i = \text{Sta. 120 to Sta. 138}$

Figure 2. Profile view along the centerline of the San Luis Dam site between stations 120 and 140.

Field investigations following the failure included visual inspections, ground surveys to measure the extent of surface displacements, installation of slope inclinometers to locate the slip surface, and collection of soil and block samples for laboratory tests. Field investigations lead to the conclusion that the clayey slopewash material in the foundation was responsible for the slide. The slopewash material is a medium to high plasticity clay (plasticity index, $PI = 17 - 21$) derived from the weathering and erosion of the sedimentary rocks at the site. Laboratory tests were performed to determine drained peak, fully softened, and residual shear strengths of slopewash material (Stark, 1987; Stark and Duncan, 1991). Peak shear strength of clay is the strength of undisturbed test specimen from the field; fully softened shear strength is the peak shear strength of reconstituted and normally consolidated clay; and residual shear strength is the minimum strength of clay after large displacements exceeding 250 mm (e.g. Duncan and Wright, 2005). Slope stability analyses of the slide showed that the shear strength of the slopewash in the foundation would have had to be reduced to its residual value for the slide to occur. This was in conflict with the accepted norm (e.g. Stark and Duncan, 1991) that the use of fully softened shear strength would be appropriate for modelling the onset of instability of this slide, i.e. for factor of safety of unity (1.0). The slope stability analyses were performed using two-dimensional (2-D) limit-equilibrium-based analysis procedures (VonThun, 1985; Stark and Duncan, 1991). Moreover, these analyses were limited to one cross section located at station 135 which was selected on the basis of surface movements (largest) in the surveyed data, and for one slip surface geometry that had been estimated from post-failure slope indicator data. The slide was about 550 m (1800 ft) long along the centreline of the dam crest (station 120 to 138). Figure 3 shows the cross sections of the dam from station 120 to station 138 in 60 m (200 ft) increments and the one at station 135; the deformed configurations of the u/s face of the dam, after the slide, are shown by dotted lines. Stations are numbered in multiples of 30 m (100 ft). Thus station 135 is 4050 m (13500 ft) from the starting point.

This slide is analysed herein using 2-D limit-equilibrium and 2- and 3-D (three-dimensional) continuum-mechanics-based procedures. The 2-D analyses are for ten cross sections shown in Figure 3. The cross section at station 126 was not available during analysis work; instead the cross section at station 135 was added because this cross section had been investigated extensively following the slide in 1981. Three-dimensional analysis is for the dam from station 120 to 138. All analyses are for fully softened and residual shear strength of the slopewash material and are for full and drawdown reservoir conditions. The drained peak shear strength was not used in the analyses because it was not an issue in the 1981 slide (Stark and Duncan, 1991). One suite of analyses was performed using an adjusted value of shear strength for the slopewash material which yields a 2-D continuum-based factor of safety of about unity for the cross section at station 135. The objectives of these analyses are to:

- compare the results from 2-D limit-equilibrium- and continuum-mechanics-based analyses;
- assess the results of 2-D models at ten cross section locations along the length of the dam;
- compare the results of 3-D analysis with those of 2-D analyses in relation to the observed movements and surface cracks, and
- draw recommendations for future analyses in dam engineering practice.

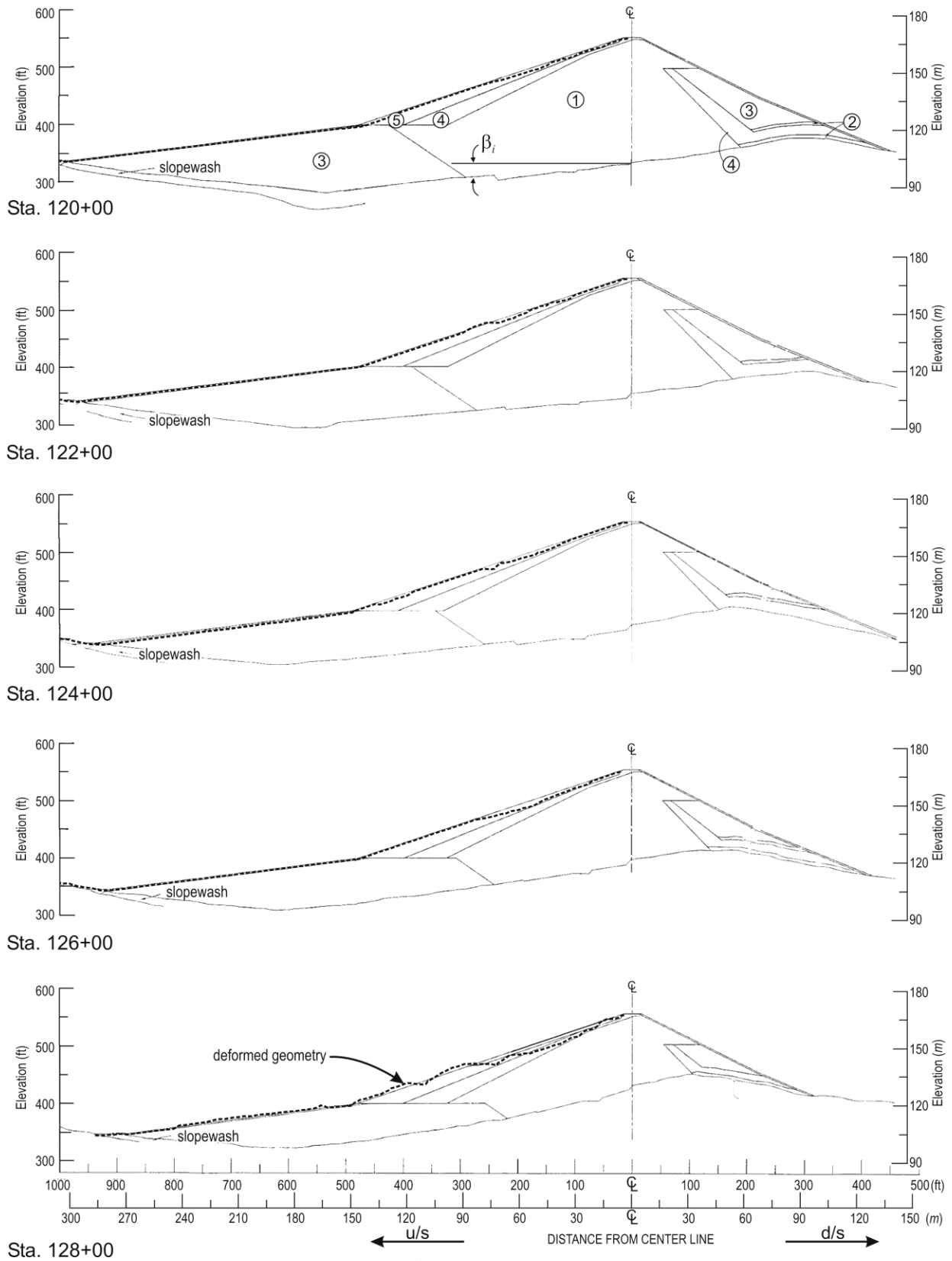


Figure 3. Cross section views of the San Luis Dam from station 120 to station 138 showing the original and deformed configuration of the dam.

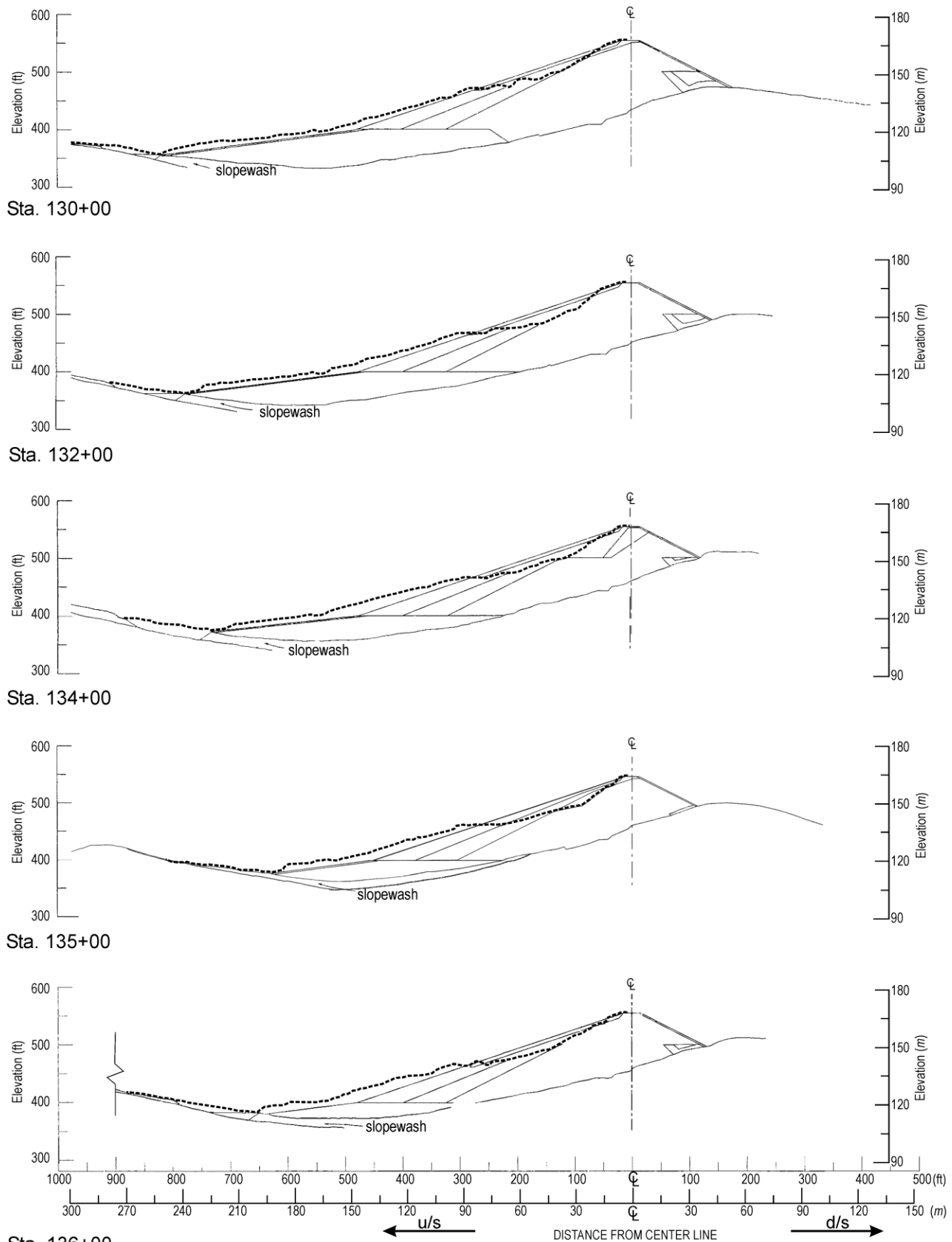
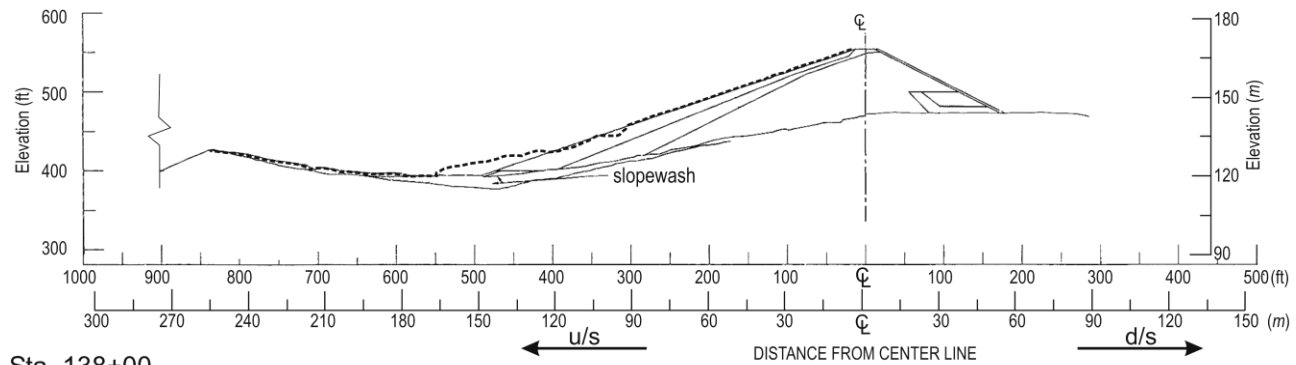


Figure 3. Continued.



Sta. station; \odot Dam zone no. for $i = 1$ to 5; β_i natural ground slope angle for $i =$ Sta. 120 to Sta. 138

Figure 3. Continued.

Limit-equilibrium-based analyses were performed using Spencer's procedure (Spencer, 1967) implemented in the computer program SSTAB2 (Chugh, 1992). Continuum-mechanics-based analyses were performed using the computer programs FLAC (Itasca, 2006) and FLAC3D (Itasca, 2002) in two- and three- dimensions, respectively. Shear strength values for materials in the dam and those of the slopewash in the foundation are as given in Stark and Duncan (1991); deformation properties are taken from typical values for similar materials (Jensen, 2010 and Duncan et al. 1980). Pore-water pressures are for piezometric surfaces for the full and rapid drawdown reservoir water levels (Mantei, 1982 and Lambe & Whitman, 1969). All materials are assumed to be elastic-perfectly plastic, the failure criterion is Mohr-Coulomb and the flow rule is assumed to be non-associative, i.e. dilation angle, ψ , = 0. The three-dimensional geometry is in a right-handed x, y, z coordinate system with the x axis along the length of the dam, the y axis in the u/s – d/s (downstream) direction, and the z-axis being vertical. Two dimensional cross sections are in y-z planes; and u, v, w refer to displacements in the x, y, z coordinate directions, respectively. The terms slide and slope failure are used interchangeably – both refer to the 1981 San Luis Dam slope instability. The term factor of safety is abbreviated as F (for limit-equilibrium) and FoS (for continuum) solutions – both refer to the factor by which the soil shear strength is divided to bring the slope to the verge of failure, i.e. F and FoS = 1.

EMBANKMENT DAM MATERIALS

The dam is a zoned earthfill embankment with the following general composition:

- zone 1 – clay, sand, and gravel as low hydraulic conductivity core
- zone 2 – sand, gravel, and cobbles
- zone 3 – shale, sandstone, conglomerate fragments, clay, silt, sand, and gravel
- zone 4 – rock fragments – 4.75 to 203 mm (3/16 to 8 inch)
- zone 5 – rock fragments – 203 to 915 mm (8 to 36 inch)

The dam zones are identified on cross section at Station 120 in Figure 3, the same zoning identification applies to all cross sections included in this figure. All materials were placed in lifts and compacted with appropriate equipment typical of the period (1963 - 1967).

Vertical permeability (K_v) of the embankment materials from the construction records of San Luis Dam are (Mantei, 1982):

- zone 1 – 2.13 cm/yr (0.07 ft/yr)
- zone 3 – 11.28 cm/yr (0.37 ft/yr).

SUBSURFACE CONDITIONS

The subsurface conditions vary along the 5.6-km (3.5-mile) length of the dam. From station 117 to station 139, the dam is founded on low hills, the crest of which lay along the axis of the dam, i.e. the natural ground slopes along the length of the dam as well as in the u/s – d/s directions (see Figures 2 and 3). These low hills are covered with locally disintegrated sedimentary rocks due to weathering which was subsequently moved due to erosion and transport, creating colluvium in the lower portions of the slope. The climate is arid and the depth of weathering on the low hills varies. Thus, in this reach of the



dam, a small amount of stripping (30 to 60 cm/1 to 2 ft) was performed before placement of embankment fill materials on what appeared to be competent foundation material (termed slopewash during field investigations of the slide). The thickness of the slopewash material varies from 1.5 m (5 ft) near the top of the hill to about 6 m (20 ft) at the base (in the u/s – d/s direction). The cut-off trench is located on the u/s side of the dam centerline.

Along the centerline of the dam, the natural ground slopes upward at about 12° from station 120 to station 130 and at about 5° from station 130 to station 136 where it transitions to near level ground and downwards thereafter. In Figure 2, this ground slope angle is marked by α . In the u/s-d/s direction, the natural ground slopes towards the upstream at different inclination angles β as shown on Figure 3 – β increases from about 5° at station 120 to about 15° at station 134, and then decreases to about 13° at station 135, and about 12° at station 138.

FIELD OBSERVATIONS OF 1981 SLIDE

1. Observations prior to the 1981 slide: Since the first filling of the reservoir in 1967, the San Luis Dam had displayed persistent, unexplained, minor cracks on the crest of the dam preceding the 1981 slide. Crest cracking had also been observed in other regions (outside the reach of the 1981 slide) where the dam was founded on similar landforms. The cracks were taken to be typical of performance of large dams after first filling of reservoir. Also, during 1975 – 1978, three significant drawdowns of the reservoir had occurred without incidence, see Figure 1(b).

2. Observations of the 1981 slide: The following field observations of the slide were noted by VonThun (1985) – see Figures 1(a), 2, and 3: First cracking occurred about 30 m (100 ft) down the u/s slope near the crest of an enveloped hill (near station 135) and progressed down the abutment towards more voluminous cross sections. The characteristics and progression of the slide mass are summarized as: (a) began as an arc-shaped crack, with ends of the arc parallel and perpendicular to the dam axis; (b) progressed from the initial length of about 150 m (500 ft) to an ultimate length of about 450 m (1475 ft); (c) took about two months to fully develop and stabilize; (d) formed a distinct pressure ridge at the toe moving over a portion of the toe of the dam for a distance of about 10 m (30 ft); and (e) moved on the order of 20 m (65 ft) with a 15 m (50 ft) vertical scarp. In view of the size of objects in Figure 1(a), the 15 m (50 ft) dimension for the vertical scarp seems to be in error (an over-estimate) – it is listed as 7.6 to 9.1 m high in Penman (1986) and 10 m high in Duncan and Wright (2005).

In terms of slide progression, Penman (1986) noted the following: The slide was first discovered on 14 September 1981 and found to be moving at 15 cm (6 in) per day. By 10 October 1981, it was moving at up to 30 cm (1 foot) per day and had formed a steep scarp 7.6 to 9.1 m (25 to 30 ft) high. The scarp was located 12 to 15 m (40 to 50 ft) upstream of the dam crest. The blacktop road on the dam crest contained cracks 25mm (1in) wide. The reservoir water level was already below the toe at this location.

LABORATORY INVESTIGATIONS

Laboratory tests of slopewash block samples from u/s and d/s resulted in the following index parameters: liquid limit ranging from 35 to 45, plastic limit ranging from 18 to 24; which yields the PI in the range 17 to 21. The preconsolidation pressure for the u/s (wetted) slopewash was estimated from oedometer tests to be in the range of 100 to 150 kPa (2 to 3 kip/ft²); this results in an over-consolidation ratio in the range of 2 to 3 in the reach of the slide. Shear strength values from direct shear tests on the slopewash are shown in Figure 4. The drained peak shear strength is $c' = 260$ kPa (5500 psf), $\phi' = 39^\circ$; fully-softened shear strength is $c' = 0$, $\phi' = 25^\circ$; and residual shear strength is $c' = 0$, $\phi' = 15^\circ$. The shear strength envelopes show large difference in the peak, fully softened, and residual shear strengths. Details of the laboratory tests are included in Stark (1987) and Stark and Duncan (1991).

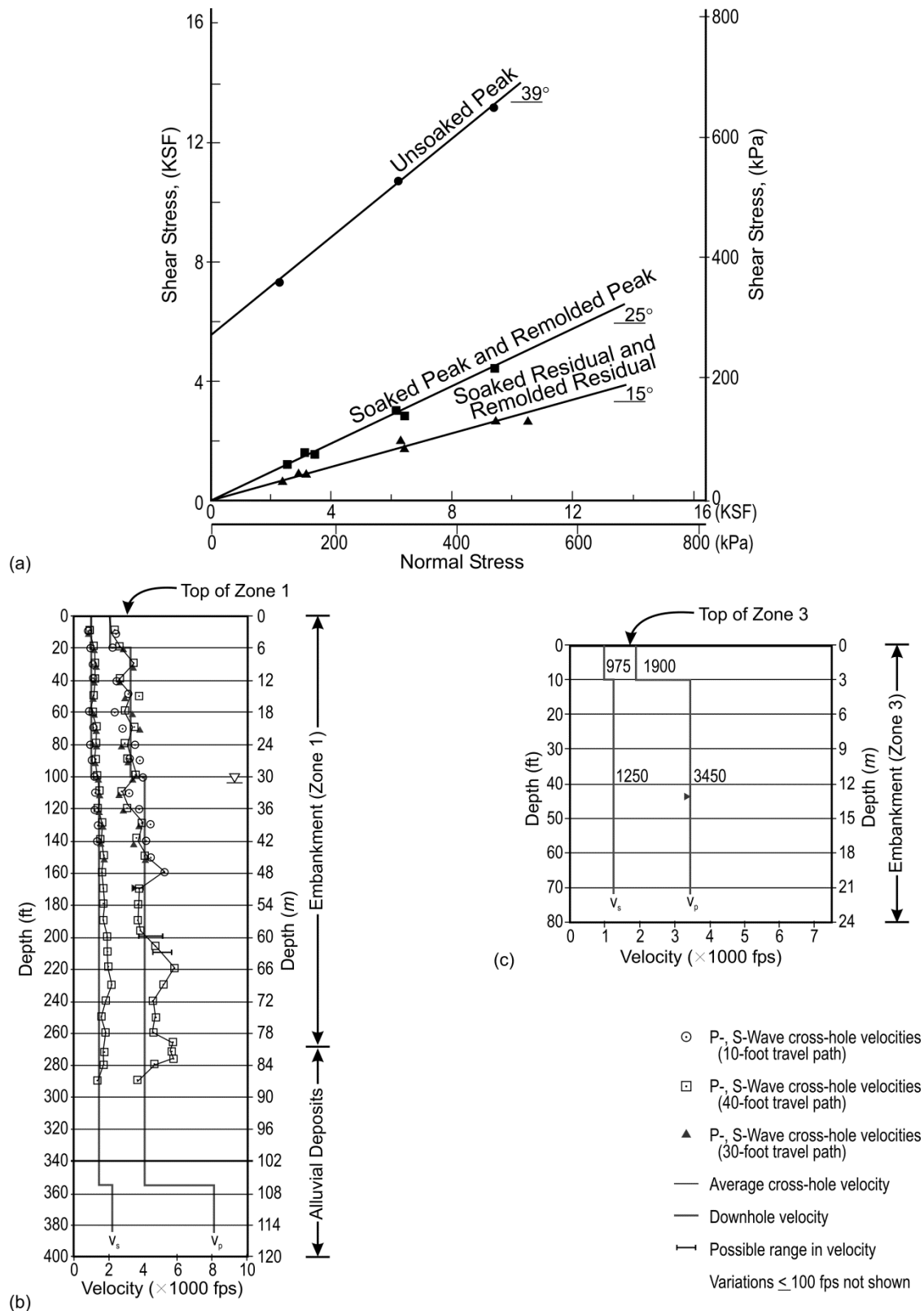


Figure 4. Material properties: (a) Shear strength descriptions of the slopewash material (Stark and Duncan 1991), reproduced with permission of ASCE; (b) and (c) Compression and shear wave profiles near the center of the dam at about station 85 (Black and Nelson, 1981), reproduced with permission of AMEC.



FAILURE MECHANISM FOR THE SAN LUIS SLIDE

Considering the details of the slopewash, sloping grounds, reservoir conditions, and field observations, the failure mechanism envisioned for the 1981 San Luis Dam slide is: (a) the buttressing effects of reservoir water pressure decreased faster than corresponding decreases in pore pressures in the dam and foundation soils; (b) effective stresses in the slopewash exceeded the shear strength at some location(s) which started the mechanism of redistribution of stresses in the dam and foundation soils, and resulted in formation of local slips; (c) the local slips connected to form a slip surface; (d) the slide mass began to move; (e) shear strength of soil at points on the slip surface decreased with increasing displacements which fueled the slide movement to continue and accelerate; and (f) the slide stopped because of: (i) more stable configuration of the slide mass; (ii) rising ground further upstream; and (iii) pore pressures dissipation because of the heat generated by the frictional sliding, etc. Thus, the failure mechanism of the San Luis Dam slide is one of progressive failure as suggested in Skempton (1964), and illustrated in Peck (1967) and Brooker and Peck (1993).

RESERVOIR WATER LEVELS

Two reservoir water level conditions of interest are (a) steady-state RWL = 165 m (540 ft) and (b) rapid-drawdown RWL = 110 m (360 ft). For RWL = 165 m, the phreatic surface was estimated from the available instrumentation data prior to the 1981 slide and calibrated 2-D finite-element-based seepage analyses of dam cross sections outside the reach of the 1981 slide (Mantei, 1982). For RWL = 110 m, the phreatic surface was assumed (due to lack of instrumented data) to rise from elevation 110 to elevation 165 along the interface between the shell and core and then follow the steady-state phreatic surface (Lamb and Whitman, 1969). Reservoir water pressure on the upstream face of the dam corresponds to the RWL condition being considered in the analysis. For illustration, Figure 5 shows the two reservoir water level conditions and associated phreatic surfaces for the cross section located at station 120; spatial layout of the reservoir and associated phreatic surface from station 120 to 138 are shown as pore pressure contours. Reservoir water loading conditions vary along the length of the slide due to changes in the ground elevations. For the RWL = 110 m condition, in locations where ground elevation is higher than elevation 110 m, there is no surface pressure due to the reservoir water.

MATERIAL PROPERTIES

Shear strength values for materials in the dam and those of the slopewash in the foundation are as used in Stark and Duncan (1991); deformation properties are based on compression and shear wave velocity profiles shown in Figure 4(b) for the San Luis Dam near station 85 (Black and Nelson, 1981) and typical values for similar materials on other dam sites (e.g. Jensen, 2010; Duncan et al. 1980). These values are shown in Table 1(a) and are used for soils that are below the phreatic surface. For soils above the phreatic surface, material properties used are shown in Table 1(b). In addition, the zone 1 material located above the phreatic surface and past the downstream edge of the dam crest was assigned $c' = 16$ kPa (350 lbs/ft²), $\phi' = 30^\circ$ to prevent occurrence of trivial slips on the downstream face of the dam.

One suite of analyses for the 2-D and 3-D continuum models was performed using an adjusted value of $c' = 0$, $\phi' = 22^\circ$ for the slopewash. This adjusted shear strength value was chosen because it gave a 2-D factor of safety of essentially unity (0.99) for the cross section at station 135 for the RWL = 110 m (360 ft) condition; the corresponding factor of safety for the 3-D case using this adjusted value is 1.08. Three-dimensional analyses were also performed to estimate the slopewash shear strength for the 3-D factor of safety to be unity for the entire reach of the slide (from Station 120 to Station 138) at the RWL = 110 m condition. A slightly lower shear strength of $c' = 0$, $\phi' = 20^\circ$ was obtained. Further details of these results are included in the analysis results section of this paper.

ITEMS OF INTEREST

Items of particular interest in this study of the 1981 San Luis Dam slope failure include (a) shear strength of slopewash at the onset of instability, (b) spatial locations of tension zones, (c) spatial geometry of the slip surface and (d) displacements of the slide mass. Also of interest are: (i) location where the failure initiated (near the crest of the dam, toe of the dam, or some-place in-between); (ii) factor of safety for the whole slide (3-D) in relation to the factor of safety for individual cross sections (2-D); (iii) spatial geometry and lateral extent of the slide, (iv) degradation of shear strength from the onset of instability to the end of slide movement (resulting from the slide displacements); and (v) rate of slide movements.

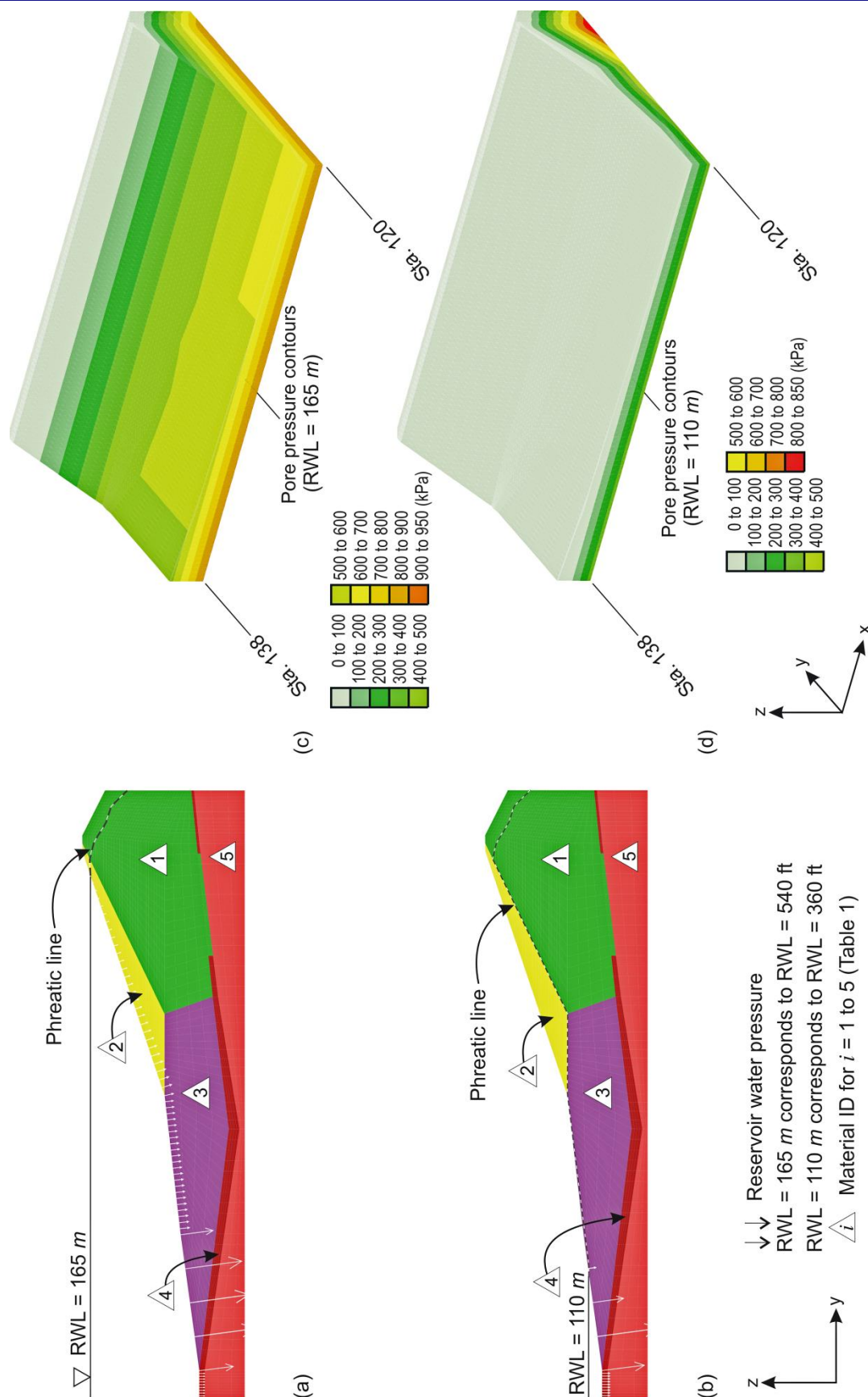


Figure 5. Reservoir water level and associated phreatic surface/pore pressure contours in the reach of the slide (used in 2- and 3-D analyses): (a) RWL = 165 m (540 ft), cross section at station 120; (b) RWL = 110 m (360 ft), cross section at station 120; (c) RWL = 165 m (540 ft), perspective view from station 120 to station 138; (d) RWL = 110 m (360 ft), perspective view from station 120 to station 138.



RATIONALE FOR THE SELECTION OF NUMERICAL ANALYSES USED

Limit-Equilibrium-Based Analysis

The 2-D limit-equilibrium based stability analyses of the San Luis Dam slide performed in 1980s were for the cross section at station 135; had used the slip surface geometry which had been estimated from the field observations and post-failure inclinometers data; and were based on a constant factor of safety assumption for the entire slip surface. Pore pressure conditions in the dam were estimated from the available instrumentation data prior to the 1981 slide and seepage analyses. In the present back-analyses of the San Luis slide, the following deviations from the standard practice were made:

1. For assessing the effectiveness of the buttress (constructed after the 1981 slide) on the stability of the San Luis Dam using 2-D limit-equilibrium method, the Spencer's procedure was modified to account for effects of pre-existing shears in the slopewash on computed factor of safety. The modification included defining a characteristic function, $f(y)$, to describe the variation of factor of safety, F , along a slip surface and finding a scalar factor, λ , which in combination with the $f(y)$ satisfies the force and moment equilibrium equations of static for the slide mass. This modification leads to a factor of safety that varies along the slip surface. For $f(y) = 1$, $\lambda = F$ which is the constant factor of safety assumption. Details of this procedure are included in Chugh (1986). In the current work, this procedure is used for the cross section at station 135 to identify the potential location where failure initiates, and where distress signs (cracks, bulges, or depressions) would be expected.
2. For assessing the lateral extent of the 1984 Carsington Dam failure using 2-D limit-equilibrium-based analyses, Skempton and Vaughan (1993) used shear forces on the lateral faces of the planar sections to distribute loads along the length of the slide in what was termed a "lateral load transfer mechanism". See Vaughan (1985, 1991) for further details of this procedure. In the current work, 3-D continuum analyses are used to determine the lateral extent of the San Luis Dam slide.

Table 1(a). Material properties below the phreatic surface.

Material ID	Unit weight, γ		Shear strength				Elastic properties *			
			Cohesion, c'		Angle of internal friction, ϕ'		Shear modulus, G		Bulk modulus, K	
	(kN/m ³)	(lbs/ft ³)	(kPa)	(lbs/ft ²)	(°)		(MPa)	(lbs/ft ²)	(MPa)	(lbs/ft ²)
1; core	20.4	130	10.5	220	25		2.4×10^2	4.9×10^6	3.9×10^3	8.1×10^7
2; shell	22.0	140	0	0	40		2.5×10^2	5.3×10^6	3.1×10^3	6.5×10^7
3; berm	21.2	135	5.3	110	25		2.5×10^2	5.3×10^6	3.1×10^3	6.5×10^7
5; rock	23.6	150	240	5000	39		1.4×10^3	3.0×10^7	1.4×10^4	3.0×10^8
4; slopewash	19.7	125	fully softened	residual	fully softened	residual	4.5×10^1	9.3×10^5	1.4×10^2	3.0×10^6
			0	0	25	15				

Table 1(b). Material properties above the phreatic surface.

Material ID	Unit weight, γ		Shear strength				Elastic properties *			
			Cohesion, c'		Angle of internal friction, ϕ'		Shear modulus, G		Bulk modulus, K	
	(kN/m ³)	(lbs/ft ³)	(kPa)	(lbs/ft ²)	(°)		(MPa)	(lbs/ft ²)	(MPa)	(lbs/ft ²)
1; core	19.5	124	10.5	220	25		2.3×10^2	4.8×10^6	5.8×10^2	1.2×10^7
2; shell	20.3	129	0	0	40		9.6×10^2	2.0×10^7	1.3×10^4	2.7×10^8



Table 1(c). Interface properties for displacement analysis.

Interface ID	Interface properties					
	Cohesion	Friction angle	Normal stiffness**		Shear stiffness**	
		(°)	kn		ks	
IF 1	0	varied during calculations from 22° → 20° → 18° → 16° → 15° → 14°	1.6×10^3	1×10^7	1.6×10^3	1×10^7

* The elastic properties of the soils were defined in terms of shear wave velocity (V_s) and Poisson's ratio (ν). The shear modulus (G) and bulk modulus (K) were calculated using the relations: $G = \gamma V_s^2 / g$ and $K = 2(1 + \nu)G / 3(1 - 2\nu)$; g is acceleration of gravity (9.81 m/s).

** The stiffness values were calculated from the elastic properties of the slopewash and the grid size therein as suggested in the program manual. Also, sliding response is known to be relatively insensitive to the stiffness values.

Continuum-Mechanics-Based Analyses

Continuum-mechanics-based 2- or 3-D analyses of the 1981 San Luis Dam slide have never been performed heretofore. However, these procedures are considered more realistic and better predictors of actual performance than just a factor of safety result obtained from limit-equilibrium-based procedures; see Griffiths and Lane (1999), Duncan (2013), Kovacevic et al. (2013). Herein, both 2- and 3-D models are used for stability and deformation analyses.

Computer Programs Used

The computer programs used in this study were largely based on their availability and past experience with their use on dam engineering projects. SSTAB2 was used for 2-D limit-equilibrium-based analyses; FLAC was used for 2-D continuum-mechanics-based analyses; and FLAC3D was used for 3-D continuum-mechanics-based analyses.

NUMERICAL MODELLING DETAILS

After the 1981 slide, detailed cross sections were developed from station 120 to 139 in increments of 30 m (100 ft). For the work included in this paper, every other cross section starting with station 120 was used. Cross section at station 135 is shown in Figures 3 and 6(a); also see Penman (1986) for additional details. The length of the 3-D model was influenced by the reach of the available cross sections. Table 2 is a summary of the details of numerical models and boundary conditions used.

The numerical scheme for determining factor of safety is termed the strength reduction procedure; its implementation in SSTAB2 is described in Chugh (2003), and for FLAC and FLAC3D in Dawson et al. (1999). In continuum-based analyses (a) tensile strength of the soil was excluded for factor of safety calculations, it was included in the displacement calculations; (b) stability analyses were in small strains, displacement analyses were in large strains; (c) gravity turn-on was used, i.e. incremental construction of the dam was not modelled; and (d) progressive character of the slide was simulated by incrementally decreasing the frictional strength of the interface from fully softened to the residual shear strength value of the slopewash; rigorous strain softening analysis for the slopewash as a function of plastic strains as suggested in Griffiths (1981) or as used in Potts et al., (1990) in 2-D finite element analysis of progressive failure of Carsington Dam was not attempted in this study because of lack of test data. Simplifications (c) and (d) used in the analyses were commensurate with the availability of good quality site-specific data.

For deformation analysis of cross section at station 135, an interface was introduced to represent slip surface in order to allow physical separation and sliding of a soil mass from its parent deposit which had happened in the San Luis slide. However, for the 3-D deformation analysis, such an interface could not be introduced because of complexities in defining the spatial geometry of slip surface as an interface. An interface is a surface on which a slide mass can slide relative to a stable base when stresses exceed the corresponding strength of the interface. In the absence of an interface, the slide mass remains tethered to the stable base which limits the amount of displacement.



Table 2. Numerical modelling details

Model	Analysis type	Discretization			Boundary conditions	Analysis procedure	Computer program used	Instructions for model development procedure
		Geometry	Number (range)					
			RWL (m)					
			165	110				
2-D limit-equilibrium	Stability	Vertical slices	25 (23-27)	20 (19-22)	Interslice force and its location for exposed face of the 1 st and last slice = 0	Spencer (for constant and variable factor of safety)	SSTAB2	User manual
2-D continuum-mechanics	Stability and deformation	Rectangular zones	1890 (1848-3296)		$v = w = 0$ on $-z$ face; $v = 0$ on $\pm y$ face	Explicit finite difference	FLAC	User manual
3-D continuum-mechanics	Stability and deformation	Brick shaped regions	50040		$u = v = w = 0$ on $-z$ face; $u=0$ on $\pm x$ face; $v=0$ on $\pm y$ face	Explicit finite difference	FLAC3D	Chugh (2013)

ANALYSIS RESULTS

Results of analyses are illustrated in individual figures. Each figure includes essential details of the model and results and is labelled to be self-explanatory. To conserve space, only introductory comments on the model and results shown in a figure are included herein which is followed by a detailed description of the most significant observations.

Limit-Equilibrium-Based Factor of Safety Results

1. Variable factor of safety: Figure 6(a) shows the model and the analysis results. The computed value of scalar parameter λ is 1.983. The average value of F is 1.005. The constant value of F is 0.99. Significant observations from the results shown in Figure 6 include:

(a) The factor of safety in the slopewash is 0.81 whereas it is greater than unity in other materials along the slip surface. This result suggests that the slope instability initiated in the slopewash material underlying the embankment.

(b) The factor of safety near the toe of the slide is about 1.3 and it is about 2.0 near the crest of the dam. This suggests that the slope instability progressed towards the toe from the slopewash; this should have resulted in a depression on the u/s slope immediately above the slopewash with $F = 0.81$ as noted in observation (a).

(c) Observation (b) is manifested by formation of cracks near the crest of the dam that occurred due to failure of the active wedge (sloping at about 45° through the zone 1 material) after the slope instability had initiated and progressed towards the toe, and F for the active wedge dropped from about 2.0 to just less than unity. Thus the formation of cracks occurred after the sliding mechanism was complete and the slide movement had initiated. This observation suggests that remediation of cracks would not have prevented the slope failure.

2. Constant factor of safety: The results for the ten cross sections for each of the two reservoir water levels and for each of the three sets of shear strength for the slopewash are shown in Table 3 and Figure 11(a). Significant observations from the results of constant factor of safety assumption include:

(a) For $RWL = 110$ m (360 ft), and residual shear strength ($c' = 0$ and $\phi' = 15^\circ$), the computed factor of safety for the cross section at station 135 is 0.994. This result agrees well with the value of unity included in Stark and Duncan (1991) and the slope failing in 1981.

(b) For the conditions identical to (a), the factor of safety for other cross sections located between stations 130 and 138 is lower than unity (range is 0.86 to 0.99) and higher than unity (range is 1.05 to 1.44) for cross sections located between stations 120 and 128. This observation raises a question about the uniqueness of the back-calculated value of $c' = 0$, $\phi' = 15^\circ$ to be representative for the slopewash in the entire reach of the 1981 San Luis Dam slide; it implies that a different value for shear strength for slopewash or pore-water pressure model would be needed if cross section at a station other than 135 is used for back-analysis.

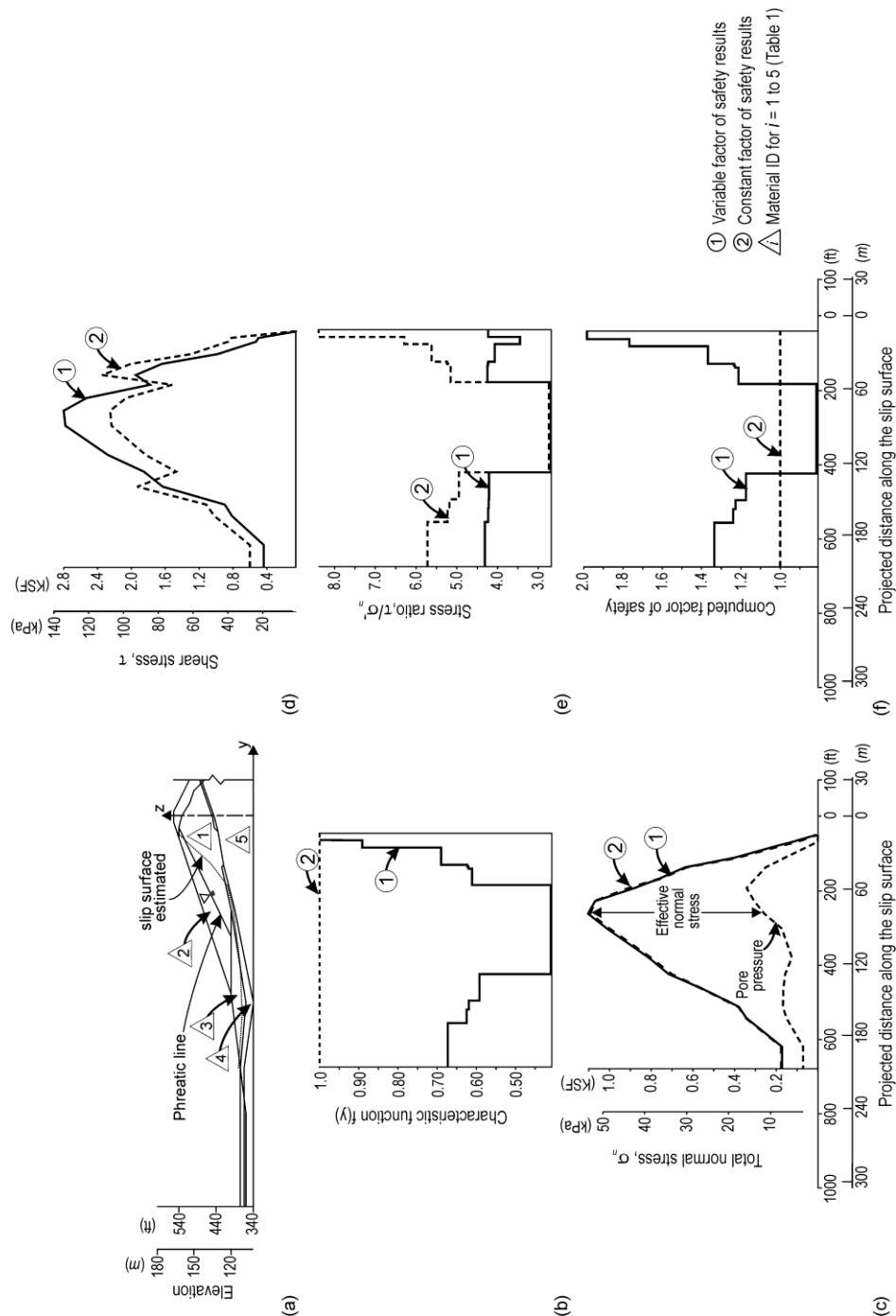


Figure 6. Limit-equilibrium based slope stability analysis results for constant and variable factor of safety for the cross section at station 135. Reservoir water level is 110 m (360 ft), angle of internal friction for slopewash is 15° , and the slip surface geometry is estimated from the post-failure field data (Stark and Duncan, 1991): (a) Cross section at Station 135; (b) Characteristic function $f(y)$ description; (c) Normal stress (σ_n) along the slip surface; (d) Shear stress (τ) along the slip surface; (e) Stress ratio (τ/σ_n) along the slip surface; (f) Factor of safety along the slip surface.

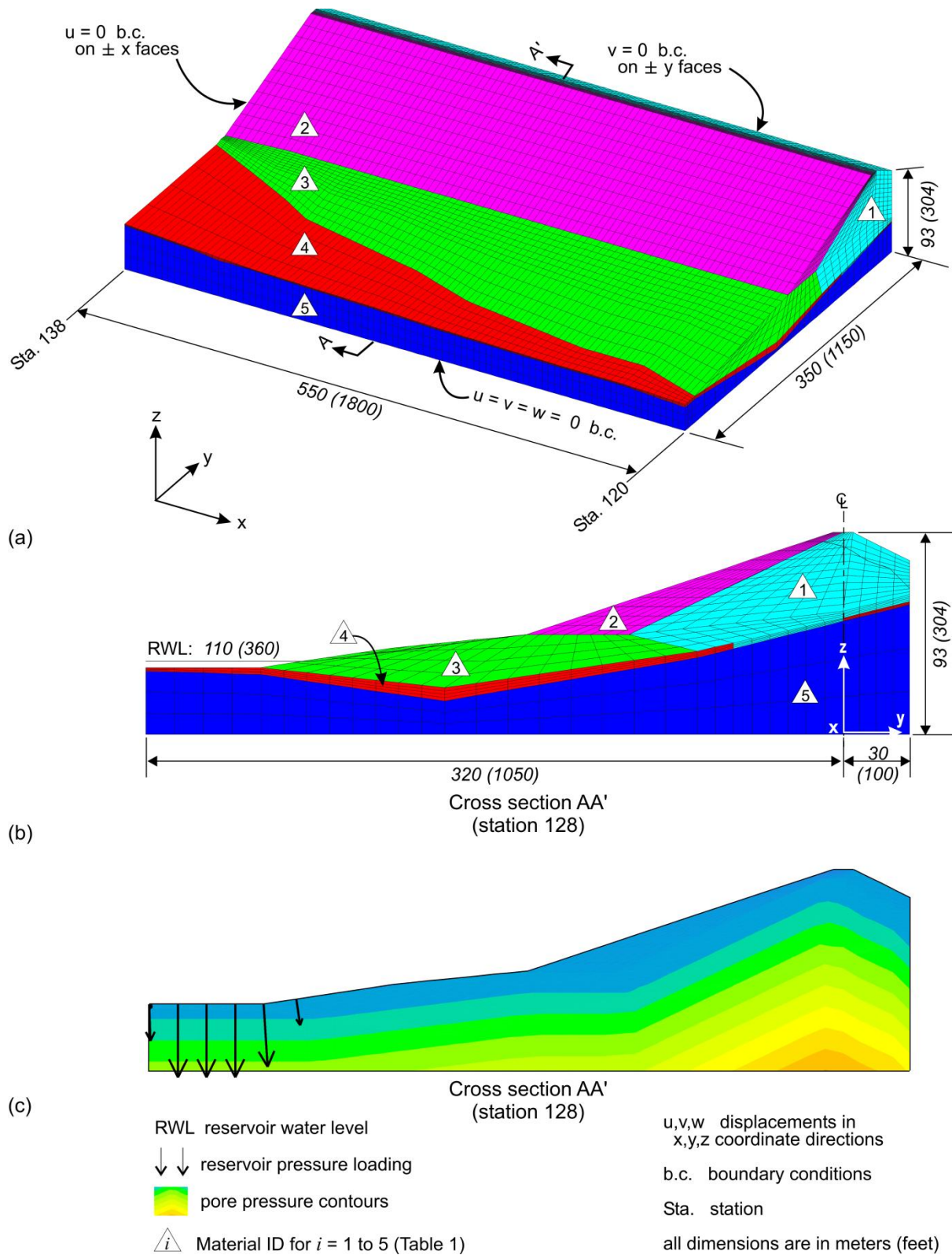


Figure 7. Numerical model of the San Luis Dam between stations 120 and 140: (a) Perspective view; (b) Cross section view at station 128; (c) Reservoir water and pore pressure for RWL = 110 m (360 ft) at station 128.



Table 3. Computed results using limit-equilibrium models†

Station	Shear strength for slopewash											
	Fully softened ($c' = 0$, $\phi' = 25^\circ$)				Adjusted value ($c' = 0$, $\phi' = 22^\circ$)				Residual ($c' = 0$, $\phi' = 15^\circ$)			
	RWL = 165 m (540 ft)		RWL = 110 m (360 ft)		RWL = 165 m (540 ft)		RWL = 110 m (360 ft)		RWL = 165 m (540 ft)		RWL = 110 m (360 ft)	
	F	δ°	F	δ°	F	δ°	F	δ°	F	δ°	F	δ°
120	3.09	-3.97	1.87	-10.3	2.86	-3.84	1.73	-9.94	2.37	-3.48	1.44	-8.65
122	2.81	-3.94	1.72	-11.0	2.59	-3.80	1.58	-10.6	2.12	-3.42	1.29	-9.42
124	2.66	-4.11	1.65	-12.3	2.44	-3.98	1.51	-11.9	1.96	-3.58	1.22	-10.7
128	2.35	-3.97	1.50	-13.2	2.13	-3.84	1.36	-12.8	1.66	-3.46	1.05	-11.5
130	2.22	-3.97	1.42	-13.0	2.00	-3.82	1.28	-12.5	1.54	-3.37	0.97	-11.1
132	2.06	-4.01	1.37	-13.6	1.86	-3.85	1.23	-13.2	1.42	-3.37	0.92	-11.8
134	1.89	-3.94	1.30	-14.7	1.70	-3.76	1.16	-14.3	1.29	-3.18	0.86	-13.0
135	1.90	-4.29	1.35	-15.4	1.76	-4.17	1.24	-14.9	1.46	-3.84	0.99	-13.4
136	1.83	-3.98	1.33	-15.7	1.65	-3.80	1.20	-15.5	1.27	-3.24	0.90	-14.9
138	1.78	-4.29	1.46	-16.0	1.59	-4.09	1.29	-15.9	1.16	-3.42	0.92	-15.2

† using Spencer's procedure; the solution is in terms of (F, δ): F is factor of safety; δ is inter-slice force inclination.

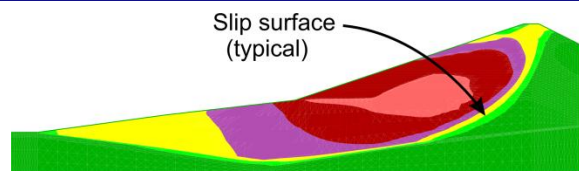
Continuum-Mechanics-Based Factor of Safety Results

Figure 7(a) shows the perspective view of the 3-D numerical model of the San Luis Dam between stations 120 and 138. Figures 7(b and c) show the cross section view of the model, the reservoir pressure loading, and the pore pressure contours for a cross section located at station 128 for RWL = 110 m (360 ft). The reservoir pressures shown in Figure 7(c) are modeled as nodal forces. The force vectors for the end-nodes are half as big as for the central nodes because the contributing area is half as big. The boundary conditions for the 2- and 3-D analyses are shown on Figure 7(a).

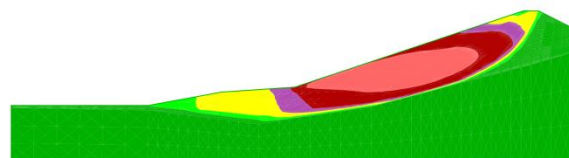
1. *2-D models:* The factor of safety results for each of the two reservoir water levels and for each of the three sets of shear strength for the slopewash are shown in Table 4 and Figure 11(b). Figure 8 shows the slip surfaces for each of the ten cross sections for RWL = 110 m and the adjusted value of shear strength for the slopewash. Significant observations based on these results include:

(a) The shear surfaces determined by the continuum analyses are different from the ones used in limit-equilibrium-based analyses.

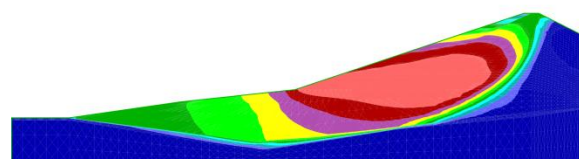
(b) For RWL = 110 m (360 ft), and residual shear strength ($c' = 0$ and $\phi' = 15^\circ$), the computed factor of safety for the cross section at station 135 is 0.69. It is also significantly less than 1.0 for all other cross sections in the reach of the 1981 slide. These results do not agree with the field data which show the severity of the 1981 slide is intense between stations 128 and 136, and it diminishes outside this range, see Figure 3.



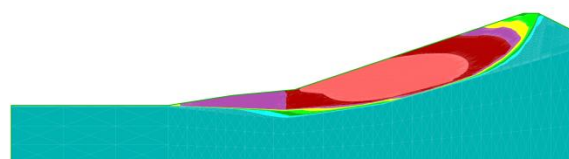
(a) Sta. 120; FoS = 1.19



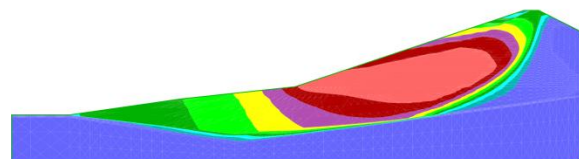
(f) Sta. 132; FoS = 1.03



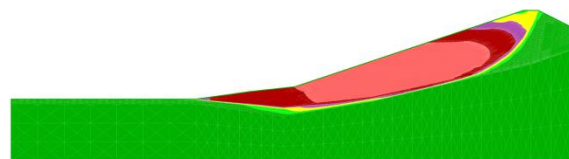
(b) Sta. 122; FoS = 1.17



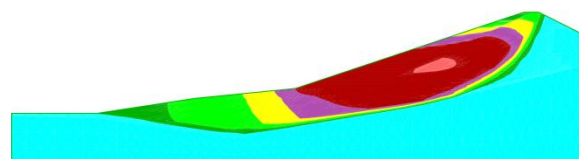
(g) Sta. 134; FoS = 1.00



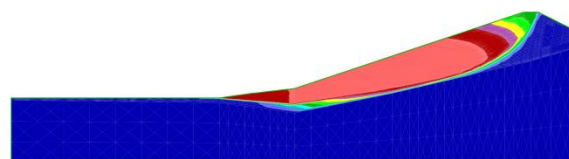
(c) Sta. 124; FoS = 1.15



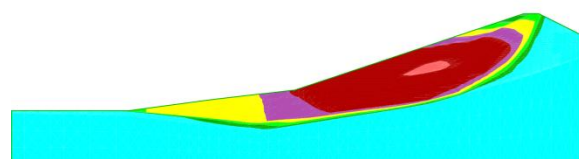
(h) Sta. 135; FoS = 0.99



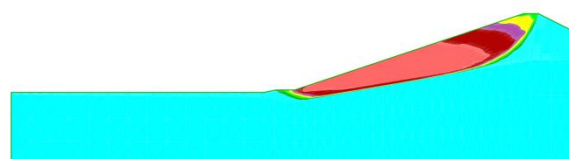
(d) Sta. 128; FoS = 1.06



(i) Sta. 136; FoS = 1.00



(e) Sta. 130; FoS = 1.01



(j) Sta. 138; FoS = 0.94

Sta. Station
FoS Factor of Safety

Figure 8. Slope stability analysis results of the two-dimensional continuum models from station 120 to station 138. Reservoir water level is 110 m (360 ft), angle of internal friction for slopewash is 22°, and the slip surface geometry is as determined by the continuum-mechanics-based computer program FLAC.



(c) For RWL = 110 m (360 ft) and an adjusted value of shear strength ($c' = 0$, $\phi' = 22^\circ$) for the slopewash, the factor of safety for the cross section at station 135 is 0.99. Also, the factor of safety for other cross sections located between stations 130 and 138 hovers around 1.0 (0.94 to 1.03) and is greater than 1.0 (1.06 to 1.19) for cross sections located between stations 120 and 128. These results agree well with the 1981 slide which had stretched between stations 120 and 138 with high intensity of distress between stations 128 and 136, and diminishing intensity outside this range – see Figure 3.

These comparisons of computed results with field data indicate that the continuum-based back-calculated value of $c' = 0$ and $\phi' = 22^\circ$ for the slopewash give a better explanation of the onset of slope failure (factor of safety = 1.0) than those obtained using limit-equilibrium with a back-calculated value of $c' = 0$ and $\phi' = 15^\circ$ do.

(d) For RWL = 110 m (360 ft) and an adjusted value of shear strength ($c' = 0$, $\phi' = 22^\circ$) for the slopewash, the shear surface for the station 135 cross section is similar to the one based on field data.

(e) No tension zone developed in any of the ten cross sections analyzed. This was concluded from an observance of the least compressive principal effective stresses.

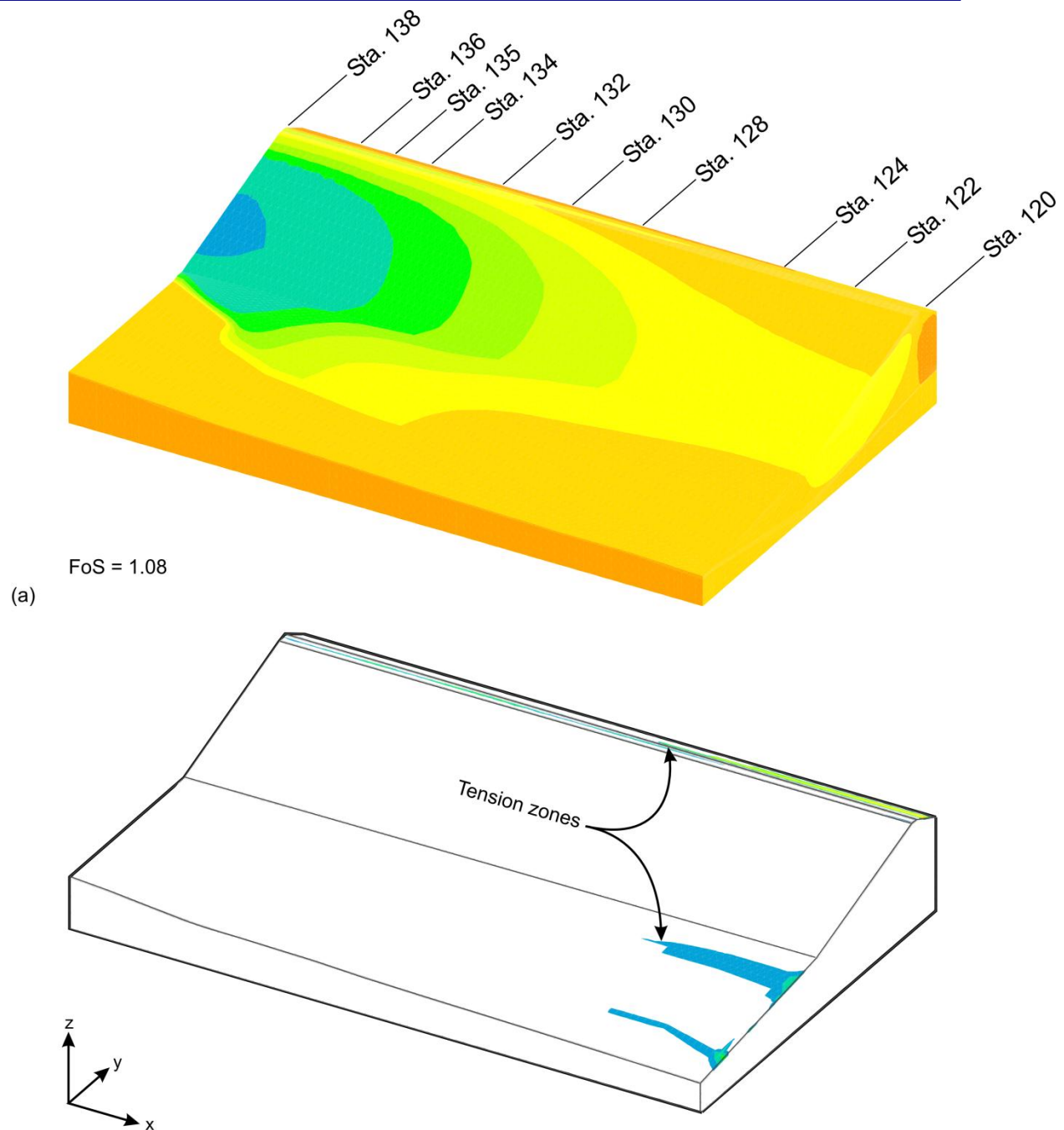
2. 3-D model: The factor of safety results for the 3-D model for each of the two reservoir water levels and for each of the three sets of shear strength for the slopewash are shown in Table 4 and Figures 11(c) and (d). The slip surface for RWL = 110 m (360 ft) and shear strength for the slopewash at adjusted values ($c' = 0$, $\phi' = 22^\circ$) is shown in Figure 9. The spatial extent of the tension zones (the least compressive principal effective stress in the range $0 \leq \sigma_3' \leq c' / \tan \phi'$) is shown in Figure 9(b). This is indicative of development of longitudinal cracks in the dam. Significant observations based on these results include:

(a) For RWL = 110 m (360 ft): the factor of safety is 1.19 for fully softened shear strength ($c' = 0$, $\phi' = 25^\circ$) of slopewash; it is 0.79 for the residual shear strength ($c' = 0$, $\phi' = 15^\circ$). Neither of these two results supports validity of associated shear strength of slopewash at the onset of slope instability.

Table 4. Computed results using continuum models†

Station	Shear strength for slopewash											
	Fully softened ($c' = 0$, $\phi' = 25^\circ$)				Adjusted value ($c' = 0$, $\phi' = 22^\circ$)				Residual ($c' = 0$, $\phi' = 15^\circ$)			
	RWL = 165 m (540 ft)		RWL = 110 m (360 ft)		RWL = 165m (540 ft)		RWL = 110 m (360 ft)		RWL = 165 m (540 ft)		RWL = 110 m (360 ft)	
	2-D FoS	3-D FoS	2-D FoS	3-D FoS	2-D FoS	3-D FoS	2-D FoS	3-D FoS	2-D FoS	3-D FoS	2-D FoS	3-D FoS
120	1.82	1.76	1.24	1.19	1.82	1.65	1.19	1.08	1.67	1.28	0.92	0.79
122	1.82		1.24		1.82		1.17		1.64		0.90	
124	1.82		1.23		1.82		1.15		1.59		0.89	
128	1.81		1.13		1.81		1.06		1.46		0.82	
130	1.79		1.10		1.78		1.01		1.36		0.76	
132	1.78		1.13		1.71		1.03		1.32		0.76	
134	1.75		1.10		1.62		1.00		1.21		0.70	
135	1.75		1.11		1.62		0.99		1.19		0.69	
136	1.70		1.10		1.55		1.00		1.14		0.71	
138	1.63		1.01		1.49		0.94		1.11		0.67	

†Using finite-difference procedures implemented in the computer programs FLAC and FLAC3D; the solution is in terms of factor of safety (FoS) and associated slip surface.



(b)

Figure 9. Slope stability analysis results of three-dimensional continuum model between stations 120 and 138. Reservoir water level is 110 m (360 ft), angle of internal friction for slopewash is 22° , and the slip surface geometry is determined by the continuum-mechanics-based computer program FLAC3D.

(a) Spatial distribution of y-displacement contours; (b) Spatial distribution of surface cracks in longitudinal direction; (c) Planar views of slip surface geometry from station 120 to station 138.

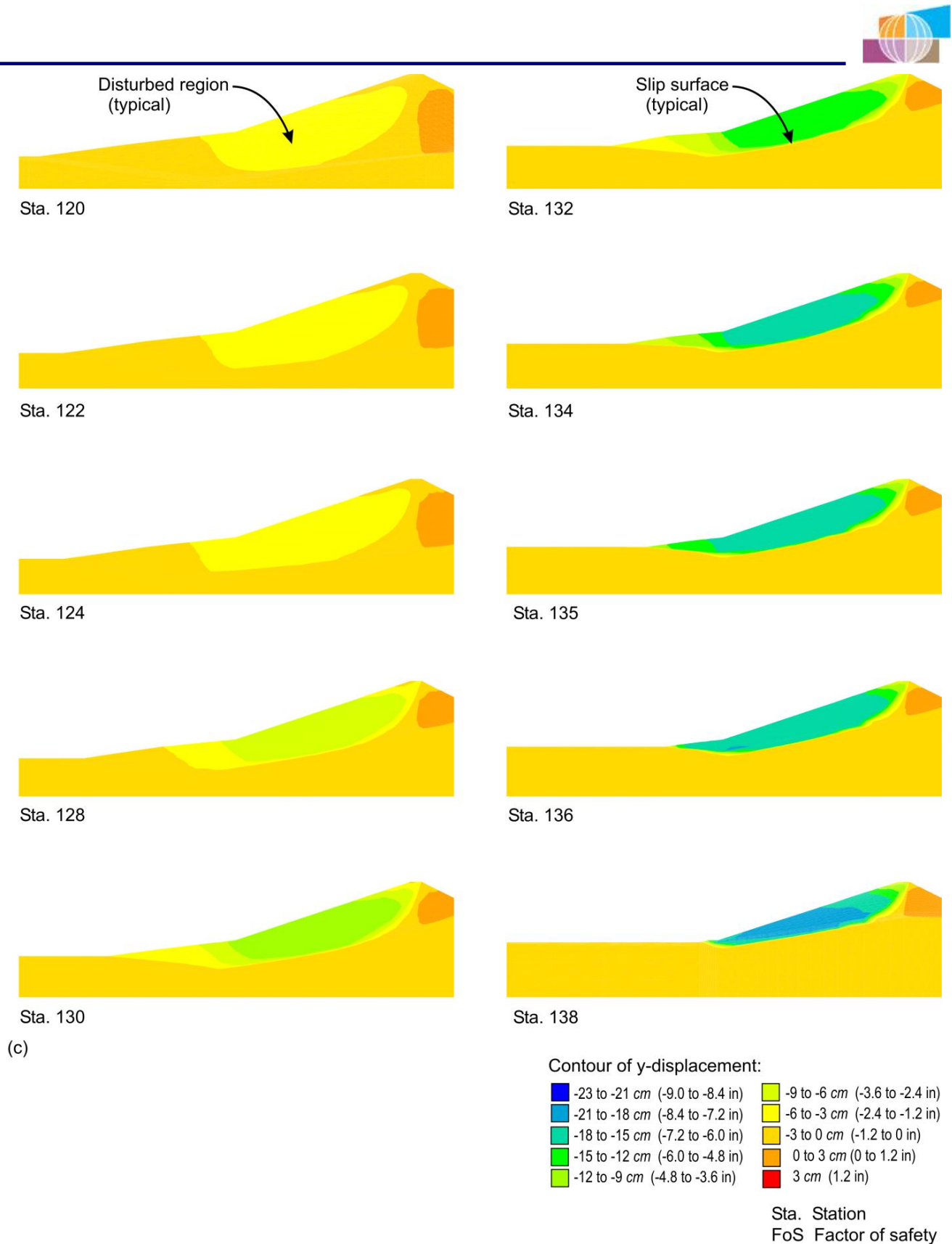


Figure 9. Continued.



(b) For $RWL = 110$ m (360 ft) and adjusted shear strength ($c' = 0$, $\phi' = 22^\circ$) for the slopewash, the factor of safety is 1.08 which is close to 1.0. For the 3-D factor of safety to be unity, the shear strength of slope wash is estimated from Figure 11(d) to be about ($\phi' = 20^\circ$, $c' = 0$). This estimated shear strength for the slopewash was checked via an additional 3-D analysis which resulted in a 3-D factor of safety = 1.01. The middle portion of the slip surface is located in the slopewash and the active and passive wedges pass through the zone 1 and zone 3, respectively. The tension zones develop near the centre of the dam crest and the scarp is arch shaped. These results compare well with the field observations and support the back-calculated value of slopewash material to be $c' = 0$ and $\phi' = 22^\circ$ (or the slightly lesser value of 20° from 3-D) at the onset of instability ($FoS = 1.0$). The difference between ($\phi' = 22^\circ$, $c' = 0$) and ($\phi' = 20^\circ$, $c' = 0$) as being representative shear strength for the slopewash is considered minor given other uncertainties and assumptions necessary in these back-analyses.

Continuum-Mechanics-Based Slope Displacement Results

1. 2-D model: The cross section at station 135 was analyzed for deformations using the 2-D slip surface shown in Figure 8(h) for the $RWL = 110$ m (360 ft), and shear strength of $c' = 0$ and $\phi' = 22^\circ$ for the slopewash. The slip surface is modelled as an interface. Adequate representation of the slip surface by the interface was verified via a factor of safety analysis of the model shown in Figure 10 with no relative sliding or separation allowed along the interface (i.e. a glued interface) which resulted in a computed factor of safety = 0.97 with a slip surface coincident with the interface. This compared well with the factor of safety of 0.99 with no interface – the small difference in FoS being due to the approximation of a continuous slip surface by a segmented line interface; in principle, they should be the same. The region above the interface is treated as an elastic-perfectly plastic medium and the region below the interface as an elastic medium. This allows the slide mass to move relative to the stable base and undergo tensile separation if required. The observation points for horizontal and vertical displacements are located on the sliding mass. The pore pressures shown act across the interface. The interface properties are shown in Table 1(c) with assumed normal and shear stiffness values. The properties for all other materials are as shown in Tables 1(a) and (b). The interface strength values (cohesion, $c' = 0$ and friction, ϕ') are decreased during deformation analysis in steps of $\Delta\phi' = 2^\circ$ until the solution procedure is unable to carry out the calculations due to bad geometry caused by large geometric distortions of the model. The pore pressures are not changed during the stepwise decreases in shear strength (slide progression). Specifically, the string of ϕ' values used is: $22^\circ \rightarrow 20^\circ \rightarrow 18^\circ \rightarrow 16^\circ \rightarrow 15^\circ \rightarrow 14^\circ$. For each setting of c' , ϕ' value, the analysis continued until the number of calculation steps exceeded the 10^6 limit. Once the slide mass begins to move, equilibrium of forces is not assured. In the analyses, the solution procedure was allowed a set number of steps to reach steady-state solution (equilibrium) at the end of which the frictional strength of the interface was decreased to the next lower value and the analysis continued. Horizontal and vertical displacements at the observation points were recorded continuously at 100 step intervals. For the cross section at station 135, the solution procedure stopped execution at $\phi' = 14^\circ$ step due to illegal geometry (due to large distortions of the model). Figure 10(c) shows the displaced configuration of the slide mass at the end of the deformation analysis ($\phi' = 15^\circ$). The v - and w -displacement histories for each of the three observation points for $15^\circ \leq \phi' \leq 22^\circ$ are shown in Figures 10(d) and (e), respectively. Figure 10(f) shows a comparison of the computed deformed geometry of the upstream face of the dam with the surveyed geometry at the same station location. Significant observations based on these results include:

(a) The computed vertical displacement at the crest of the dam is about 5 m (18 ft), and horizontal displacement near the toe of the slide is about 4.5 m (15 ft). The field data are: 8 to 10 m (25 to 30 ft) for the vertical scarp near the crest of the dam, and 10 m (30 ft) for the horizontal displacement at the toe. This aspect of comparison between the field data and computed results is considered 'fair' considering the uncertainty in the numerical values included in VonThun (1985).

(b) For the rate of sliding, the results shown in Figs. 10(d) and (e) are interpreted in relative terms, since there is no involvement of time in the analyses performed. The horizontal (v) and vertical (w) displacements at the observation points increase from almost null for $\phi' = 22^\circ$ to their maximum value for $\phi' = 15^\circ$ in different increments over the same number of calculation steps. For $\phi' = 15^\circ$, the computed rate of sliding towards the upstream, after the initial start of observable displacement (corresponding to $\phi' = 20^\circ$), is at about one-and-a-half to two times as fast as at the start. This range is calculated using the rates of v and w displacements at the observation locations shown on Figure 10(a) and are with respect to the number of computation steps (i.e. slopes of the lines shown in Figures 10(d) and (e)). The field data on the rate of slide movements are: 15 cm per day on 14 September 1981 to up to 30 cm per day by 10 October, 1981 (i.e. twice as fast as at the start). This comparison between the computed results and the field data is considered 'good'.

(c) The overall comparison of the computed and observed deformed geometry of the upstream face of the dam shown in Figure 10(f) is considered 'poor'. It is discussed further in the next section.

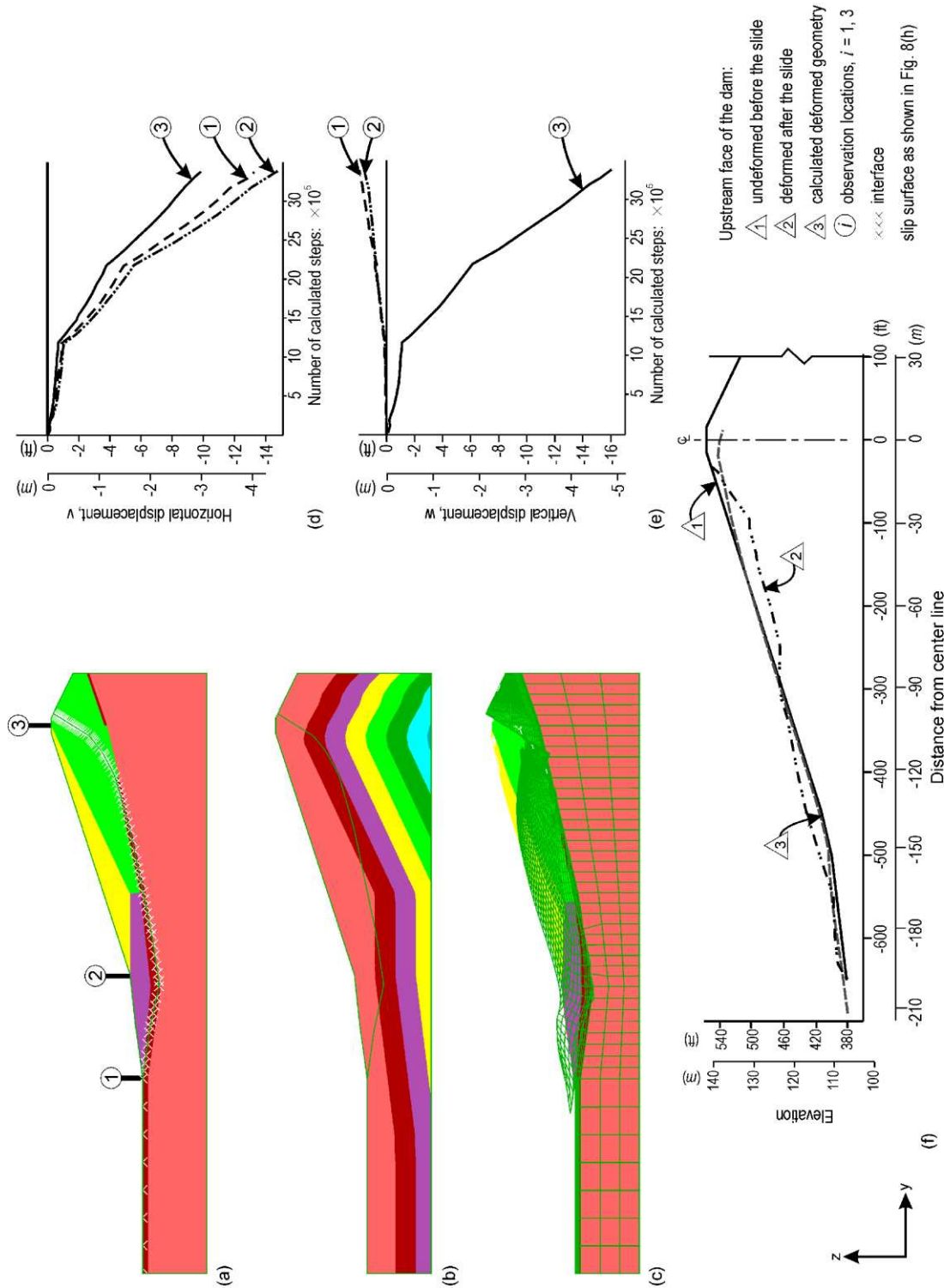


Figure 10. Displacement analysis results for the cross section at station 135. Reservoir water level is 110 m (360 ft), angle of internal friction for slope wash is decreased from 22° to 14° in steps of 2° with numerical instability occurring at friction angle of 14°; the slip surface geometry is as shown in Figure 8(h). The slip surface is modeled as an interface in the continuum-mechanics-based computer program FLAC: (a) Model set-up; (b) Pore pressure contours; (c) Deformed geometry (magnified 5x) at friction angle = 15° for the interface; (d) Horizontal (v) displacement history for friction angle from 22° to 15°; (e) Vertical (w) displacement history for friction angle from 22° to 15°; (f) Computed and surveyed geometry of the upstream face of the dam.



2. *3-D model:* The 3-D deformation analysis was performed assuming failure had initiated in the slopewash between stations 134 to 136 and then spread laterally via the load transfer mechanism. This was accomplished by reducing the shear strength of the slopewash between stations 134 to 136 in increments of 2° and holding the strength elsewhere at its adjusted value of ($c' = 0$ and $\phi' = 20^\circ$); the pore pressures are not changed during the stepwise decreases in shear strength (slide progression). Figure 12 shows the model and deformed geometry of the dam (magnified 100 \times). The pattern of deformed geometry is similar to the one observed in the field, i.e. deformations begin to increase from station 124 forward, reach their maximum near station 135 and then decrease. However, the magnitude of deformations is very small because of tethering to the stable base as explained earlier.

DISCUSSION OF RESULTS

The results from stability and deformation analyses presented demonstrate a fairly consistent agreement with the observed features of the 1981 San Luis Dam slide. The 3-D deformation results can be improved by modelling true strain-softening behaviour of slopewash. The following comments are a summary discussion of results from individual groups of analyses:

(a) The limit-equilibrium-based factor of safety results shown in Figure 11(a) show a spike at station 135, in an otherwise smooth decrease from station 120 to station 138, for each of the two reservoir water levels and each of the three strength values for the slopewash. This observation has two aspects: (i) the smooth character of the plot validates fairly consistent projection of the estimated shear surface geometry for station 135 at cross sections located at other stations; and (ii) there is something unique about the cross section at station 135 which causes the factor of safety to be higher than that at neighbouring cross sections, say at stations 134 and 136. It should be noted that the dam cross section at station 135 is smaller than the cross sections at stations 134 and 136 – this results in a smaller destabilizing force at station 135; however, the resisting forces at these near-by stations are identical (because of identical shear surface). This results in a higher factor of safety against sliding failure at station 135 as compared to the corresponding values at stations 134 and 136. A similar spike is also displayed, to a smaller scale, in the 2-D continuum-based results shown in Figure 11(b).

(b) Limit-equilibrium-based factor of safety results shown in Figure 11(a) for RWL = 110 m (360 ft) and residual shear strength ($c' = 0$, $\phi' = 15^\circ$) for the slopewash give factor of safety of 1.0 only for the cross section at station 135. Projecting the estimated shear surface on other cross sections (in the neighbourhood of station 135) gives factors of safety which are considerably less than unity. This result does not support the general conclusion that the San Luis Dam slide initiated at the residual strength of the slopewash (Stark and Duncan, 1991). Furthermore, if the slide did initiate at $c' = 0$, $\phi' = 15^\circ$, there should occur additional loss of shear strength due to the slide displacements. This contradicts the laboratory test data which determined $c' = 0$, $\phi' = 15^\circ$ as the residual shear strength of slopewash.

(c) Using $c' = 0$ and $\phi' = 22^\circ$ as the representative shear strength of the slopewash in the 2-D continuum-models for RWL = 110 m (360 ft), the computed factors of safety are consistently ≈ 1.0 (0.94 to 1.03) for cross sections located between stations 130 and 138, see Figure 11(b). The factor of safety values increase steadily from station 128 to station 120 (1.06 at station 128 to 1.19 at station 120); see Figure 11(b). These results are in general agreement with the field data shown in Figure 3 which show high severity of distress between stations 128 and 136 and gradually diminishing severity outside this range. It is inferred from this observation that the San Luis Dam slide likely initiated at the $c' = 0$ and $\phi' = 22^\circ$ as the shear strength for slopewash.

(d) From the continuum-based 3-D stability analyses, the back-calculated shear strength value for the slopewash (at the onset of instability for the total length of the model) is $c' = 0$ and $\phi' = 20^\circ$. This value is reasonably close to the laboratory determined fully softened value of $c' = 0$ and $\phi' = 25^\circ$. This also agrees well with Skempton's recommendation that use of fully softened shear strength for onset of slope failures (FoS = 1) in highly plastic clays is appropriate. The small difference in ϕ' (25° measured versus 20° back-calculated) for the slopewash is likely due to the variability in the slopewash and (or) involvement of dam zone materials in the San Luis Dam slide.

(e) The continuum-based 2-D deformation analysis (with an interface) results are in reasonable agreement with the surveyed displacement data after the slide. There is no time factor in the displacement calculations, however, in relative terms, the rate of displacements estimated from computed results (one-and-half to two times as fast towards the end of sliding as at the start) is similar to the one observed in the field data (two times as fast towards the end of sliding as it was at the start).

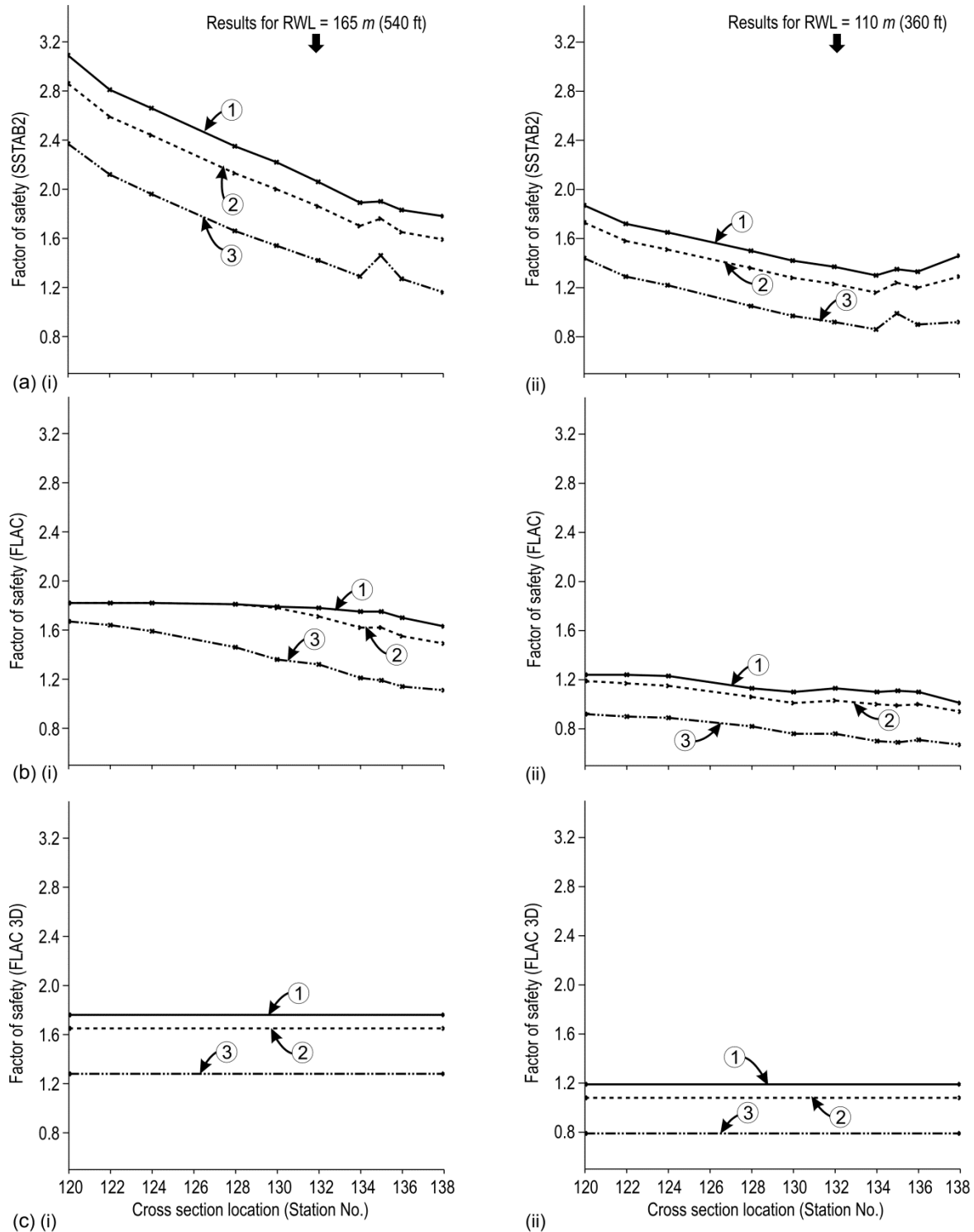


Figure 11. Summary plot of computed factor of safety results in the reach of the slide:
 (a) Computed results from SSTAB2: (i) RWL = 165 m (540 ft), (ii) RWL = 110 m (360 ft);
 (b) Computed results from FLAC: (i) RWL = 165 m (540 ft), (ii) RWL = 110 m (360 ft);
 (c) Computed results from FLAC3D: (i) RWL = 165 m (540 ft), (ii) RWL = 110 m (360 ft);
 (d) Computed results from FLAC3D: (i) RWL = 165 m (540 ft), (ii) RWL = 110 m (360 ft).

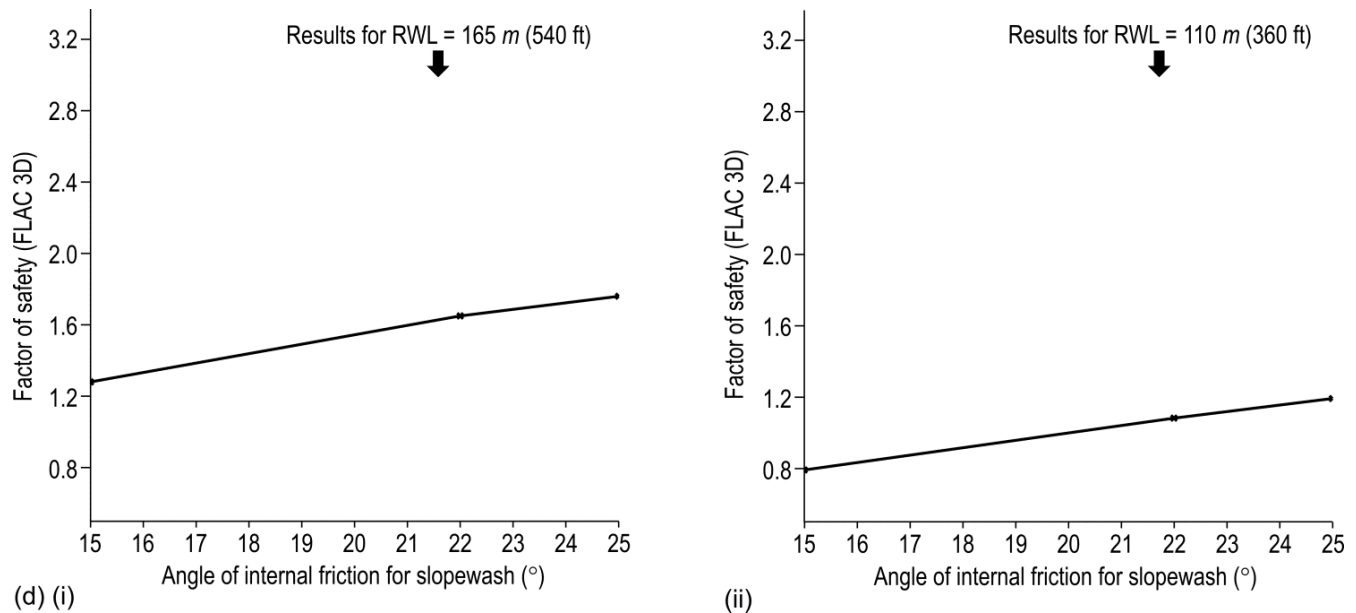


Figure 11. Continued.

(f) The 3-D deformation results shown in Figure 12, in principle, are in agreement with the lateral load transfer mechanism envisioned in Skempton and Vaughan (1993). While the computed pattern of deformations for the u/s face of the dam is similar to the signs of distress observed in the field after the slide, the magnitude of computed deformations is very small compared to the surveyed data.

Uncertainties in the Analyses

- (a) The thickness of the slopewash and its spatial distribution (location and extent) are estimates based on limited site investigation data.
- (b) Pore pressures for the drawdown condition is assumed and not based on instrumented data.
- (c) Simulation of the strain softening character of the slopewash is rudimentary.

Aspects of the 1981 Slide not Included in the Analyses

Possible effects of (a) cracks on the crest of the dam observed prior to the 1981 slide, and (b) earlier significant drawdowns of the reservoir (1975 – 1978) on (c) progressive character of the 1981 slide. These three items are likely linked in that (c) was a continuation of (a and b) which culminated in the occurrence of the 1981 slide. However, it is only a hypothesis for which different scenarios can be conceptualized to describe the link. Also, the dynamics of the moving mass must have contributed to the final displaced configuration of slid materials. The analyses included herein simply demonstrate that at the onset of instability, the mobilized strength in the slopewash is higher than the residual value and that it approaches the residual strength during the sliding due to large displacements of the slide mass.

RECOMMENDATIONS FOR ENGINEERING PRACTICE

1. In studying slope failures with all their complexities, it is best to use observational skills to get to the essential details of the problem. For the San Luis Dam slope failure, the field observations and the laboratory testing performed after the slide proved to be useful in making the numerical assessments included in this paper.

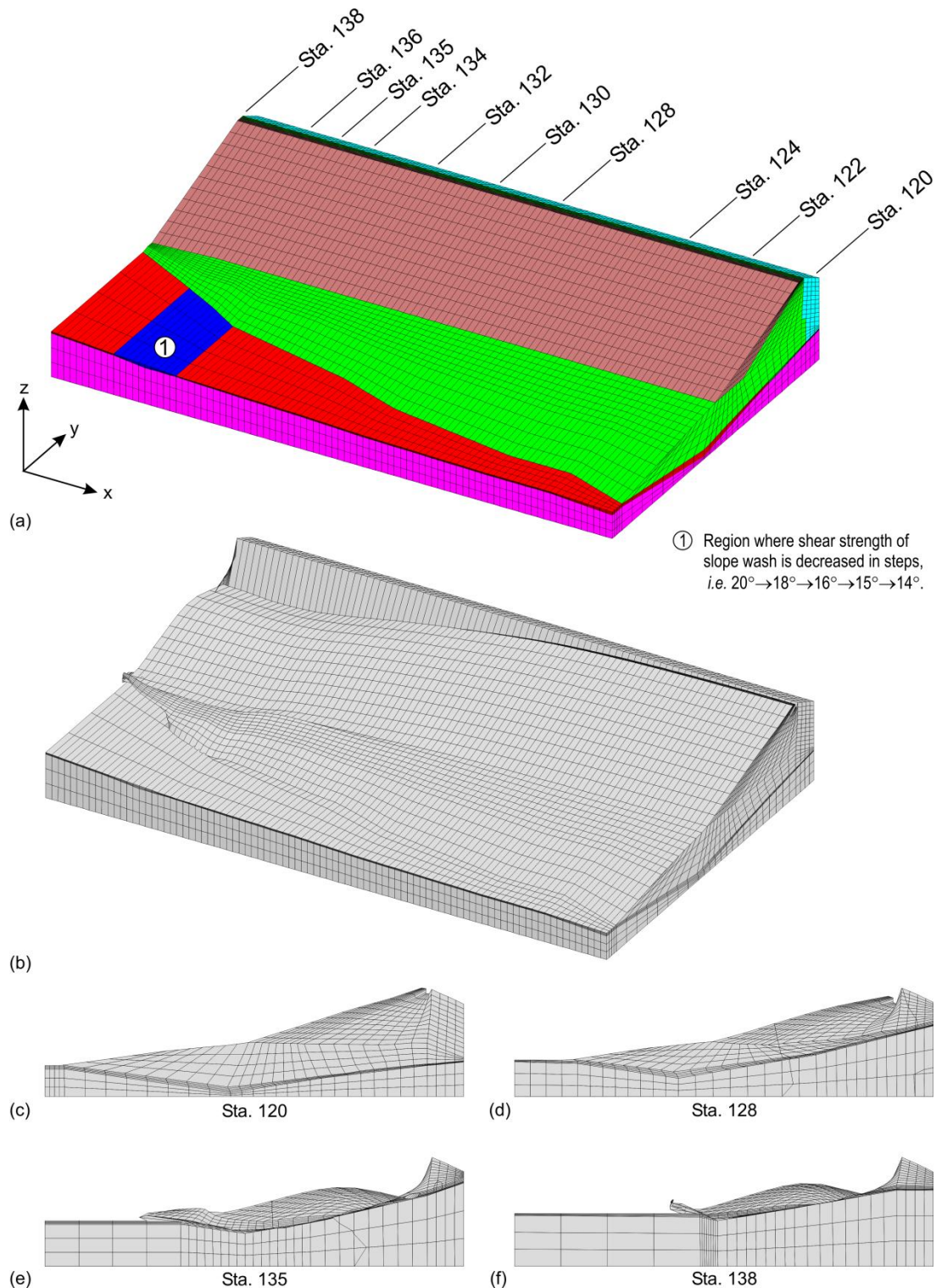


Figure 12. Computed displacement results (effects of lateral load transfer and progressive failure simulation) for the three-dimensional continuum model between stations 120 and 138. Reservoir water level is 110 m (360 ft). Angle of internal friction (ϕ') for slopewash from station 134 to 136 is decreased in steps, ($20^\circ \rightarrow 18^\circ \rightarrow 16^\circ \rightarrow 15^\circ \rightarrow 14^\circ$). (a) Assumed region of progressive failure in slopewash; (b) spatial extent of deformed geometry (magnified 100 \times) for $\phi' = 15^\circ$; (c) to (f) planar views of the deformed geometry (magnified 100 \times) at station 120, 128, 135, and 138, respectively.



2. For complex natural ground topography, a 3-D slope stability analysis is suggested. There is no simple alternative in terms of using 2-D slope stability analysis results either in terms of taking an average value or using a multiplier to estimate the 3-D factor of safety. For the San Luis Dam slide, the 3-D factor of safety cannot be estimated correctly from a single 2-D plane strain analysis.

3. Adequacy of soil properties determined from back-analyses of a slope failure should be verified by other independent means prior to accepting them as being representative for locations other than the 2-D cross section used for back-analysis.

CONCLUDING REMARKS

1. The paper has demonstrated that a relatively simple elastic plastic model with a Mohr-Coulomb failure criterion is successful in explaining the mechanisms involved in the 1981 San Luis Dam slope failure using published soil strength parameters. Limit-equilibrium-based stability analyses, while simple and computationally efficient are unable to explain the San Luis Dam slide in its entirety.

2. While the results reported in this paper captured the essence of stability aspects of the San Luis Dam slide, the match for the displaced geometry of the upstream face of the dam left room for improvement. Better characterisation of the deformation parameters of the dam materials is required to improve on these results.

3. With the exception of the back-calculated slope wash shear strengths of $\phi' = 22^\circ$ and $c' = 0$ for 2-D (station 135), and $\phi' = 20^\circ$ and $c' = 0$ for 3-D, no attempt was made to calibrate the numerical models to achieve a match with the field data. The current work presented results that used a systematic approach involving available dam cross sections, reservoir operations, and previously reported material properties.

ACKNOWLEDGEMENTS

The authors would like to express their sincere thanks to Dr. Zorica Radakovic-Guzina for her interest and helpful communications on the subject matter of this paper, and to Cindy Gray for her assistance in preparing the graphics for this paper.

REFERENCES

- Black, W. E. and Nelson, J. S. (1981). Geophysical investigations, San Luis Dam, Los Banos, California, Harding-Lawson Associates, Novato, California.
- Brooker, E. W. and Peck, R. B. (1993). Rational design treatment of slides in over consolidated clays and clay shales. *Canadian Geotechnical Journal*, 30(3): 526-544.
- Chugh, A. K. (1986). Variable factor of safety in slope stability analysis. *Geotechnique*, 36(1): 57-64.
- Chugh, A. K. (2003). On the boundary conditions in slope stability analysis. *International Journal for Numerical and Analytical Methods in Geomechanics*, 27(11): 905-926.
- Chugh, A. K. (1992). User information manual for slope stability analysis program SSTAB2. U.S. Bureau of Reclamation, Denver, Colorado.
- Chugh, A.K. (2013). Development of three-dimensional numerical models for dams. In proceedings of the International Commission On Large Dams (ICOLD) 2013 Symposium on Infrastructure Development to Infrastructure Management, Seattle, Washington: 449-460.
- Dawson, E. M., Roth, W. H., and Drescher, A. (1999). Slope stability analysis by strength reduction. *Geotechnique*, 49(6): 835-840.
- Duncan, J.M. (2013). Slope stability then and now. In proceedings of the Geo-Congress 2013: Stability and Performance of Slopes and Embankments III. ASCE, Geotechnical Special Publication No. 231: 2191-2210.
- Duncan, J. M., Byrne, P., Wong, K. S. and Mabry, P. (1980). Strength, stress-strain and bulk modulus parameters for finite element analyses of stresses and movements in soil masses. Geotechnical Engineering Research Report No. UCB/GT/80-01, University of California, Berkeley, California.
- Duncan, J. M. and Wright, S. G. (2005). Soil strength and slope stability. Wiley, Hoboken, New Jersey.
- Griffiths, D. V. (1981). Computation of strain softening behaviour. In proceedings of the Symposium on Implementation of Computer Procedures and Stress-Strain Laws in Geotechnical Engineering, Chicago, U.S.A., (editors: C. S. Desai and S. K. Saxena), Vol. II, pp. 591-604, Acorn Press.
- Griffiths, D. V. and Lane, P. A. (1999). Slope stability analyses by finite elements. *Geotechnique*, 49(3): 387-403.
- Itasca Consulting Group. FLAC3D – Fast Lagrangian Analysis of Continua in 3 Dimensions. Itasca Consulting Group, Minneapolis, Minnesota, 2002.



-
- Itasca Consulting Group. FLAC – Fast Lagrangian Analysis of Continua. Itasca Consulting Group, Minneapolis, Minnesota, 2006.
- Jensen, N. (2010). Scoggins Dam issue evaluation: FLAC deformation analyses. Technical Memorandum No. OI-86-68311-8. U.S. Bureau of Reclamation, Denver, Colorado.
- Kovacevic, N., Hight, D. W., Potts, D. M. and Carter, I. C. (2013). Finite-element analysis of the failure and reconstruction of the main dam embankment at Abberton Reservoir, Essex, UK. *Geotechnique*, 63(9): 753-767.
- Lambe, T. W. and Whitman, R. V. (1969). *Soil Mechanics*. Wiley, New York.
- Mantei, C. L. (1982). Pore pressure study, San Luis Dam. Technical memorandum No. SL-III-230-7, U.S. Bureau of Reclamation, Denver, Colorado.
- Peck, R. B. (1967). Stability of natural slopes. *Journal of the Soil Mechanics and Foundation Division, Proceedings of the American Society of Civil Engineers*, 93(4): 403-417.
- Penman, A. D. M. (1986). On the embankment dam. *Geotechnique*, 36(3): 303-348.
- Potts, D. M., Dounias, G. T. and Vaughan, P. R. (1990). Finite element analysis of progressive failure of Carsington embankment. *Geotechnique*, 40(1): 79-101.
- Skempton, A. W. (1964). Long term stability of clay slopes. *Geotechnique*, 14(2): 75-102.
- Skempton, A. W. and Vaughan, P. R. (1993). The failure of Carsington Dam. *Geotechnique*, 43(1): 151-173.
- Spencer, E. (1967). A method of analysis of the stability of embankments assuming parallel interslice forces. *Geotechnique*, 17(1): 11-26.
- Stark, T. D. (1987). Mechanism of strength loss in stiff clays. Ph.D. dissertation. Virginia Polytechnic Institute and State University, Blacksburg, Virginia.
- Stark, T. D. and Duncan, J. M. (1991). Mechanism of strength loss in stiff clays. *Journal of Geotechnical Engineering*, 117(1): 139 – 154.
- Vaughan, P. R. (1985). On questions raised by the investigations into the Carsington Dam Slide: discussion panel on Geological aspects of slope stability problems. In proceedings of the 11th International Conference on Soil Mechanics and Foundation Engineering, San Francisco, 5: 2817-2818.
- Vaughan, P. R. (1991). Stability analysis of deep slides in brittle soil: lessons from Carsington. In proceedings of the International Conference on Slope Stability Engineering, pp. 1-11. London: Thomas Telford.
- VonThun, J. L. (1985). San Luis dam upstream slide. In proceedings of the 11th International Conference on Soil Mechanics and Foundation Engineering, San Francisco, 5: 2593-2598.

**The International Journal of Geoengineering Case Histories
(IJGCH) is funded by:**



Email us at main@geocasehistoriesjournal.org if your company wishes to fund the ISSMGE International Journal of Geoengineering Case Histories.

The open access Mission of the International Journal of Geoengineering Case Histories is made possible by the support of the following organizations:



Access the content of the ISSMGE International Journal of Geoengineering Case Histories at:
<https://www.geocasehistoriesjournal.org>